Dark Matter detection and measurement through Weak Lensing

Application to the Cluster of Galaxies Abell 209

V. Antonuccio-Delogu, S. Paulin-Henriksson

INAF – Catania Astrophysical Observatory, ITALY

M. Radovich, A. Mercurio, C. Haines, G. Busarello, P. Merluzzi

INAF – Capodimonte (Naples), IT

U. Becciani INAF – Catania , IT

COSMOCT: "*Cosmology and Computational Astrophysics at Catania Astrophysical Observatory*"

- Sponsored under Marie-Curie *Transfer-of-Knowledge* action (VI FP)
- Partners: Dept. of Astroph., Oxford/J. Silk, AI Potsdam/ S. Gottloeber

- MC Postdoctoral fellow: S. Paulin-Henriksson (→ 12/2006)

Microlensing → KSB++ pipeline for WL analysis

- Short-term visitors program (MHD, Galactic dynamos)

Velocity Dispersion of Matter of Cluster galaxies

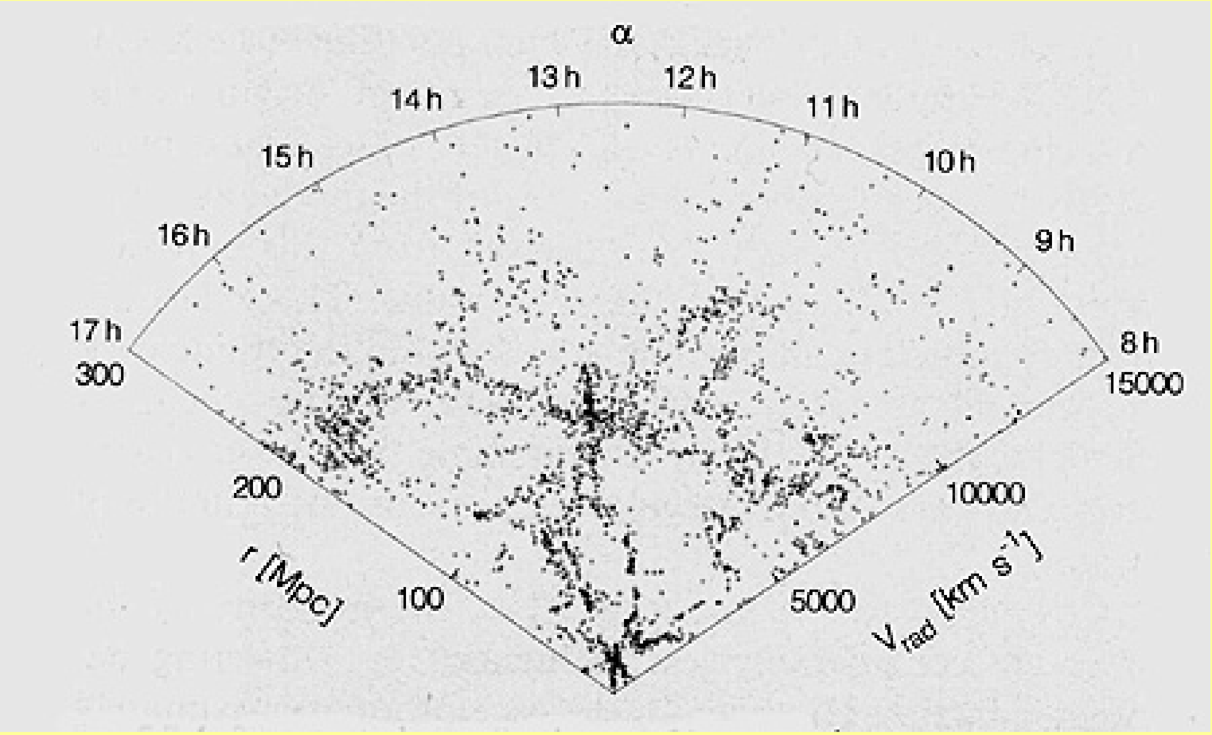

- In a wedge diagram where angular position θ is plotted against radial recession velocity v_{rad} (both measurable) Clusters of galaxies are seen as <u>extended regions</u>
- Galaxies in clusters have chaotic motions because they are in equilibrium within the Dark Matter potential well

Dark Matter in Clusters

- Main evidences:

a) Velocity dispersion of galaxies: sigma_v >approx 10^3 Km/sec within R=1.5 Mpc h^{-1} (h = H_0/100 Km/sec/Mpc)

$$\langle v \rangle^2 = \frac{G M_{dyn}(R)}{R}$$

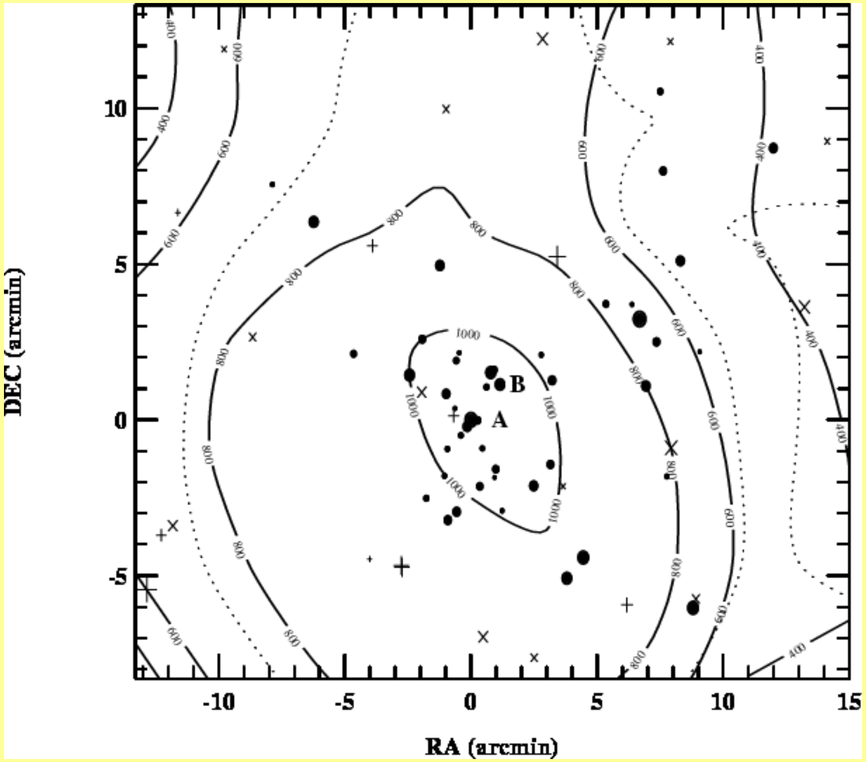

Abell 970 (Sodre' et al, 2001)

- For A970 this gives $\langle v \rangle^2$ approx 3.48×10^{17} M_{sol}

- NOTE: Assumed that *galaxies* are representative of *Dark Matter* distr., and Spher. distr. assumed

- Lokas et al. (2006) for 3D detailed anal. of vel. dist. in A1689

Dark Matter in Clusters (cont.)

b) Hard (> 10 keV) X-ray emission from Intergalactic Gas

Abell 754 / Keck Telescope Archive

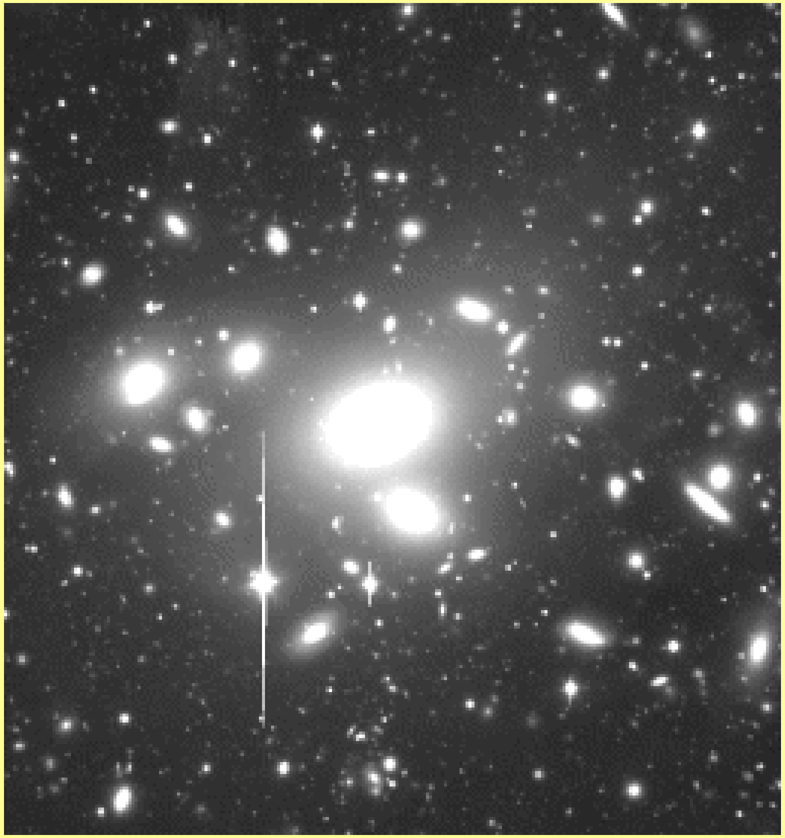

Abell 754/ ROSAT (Boehringer et al., 1999)

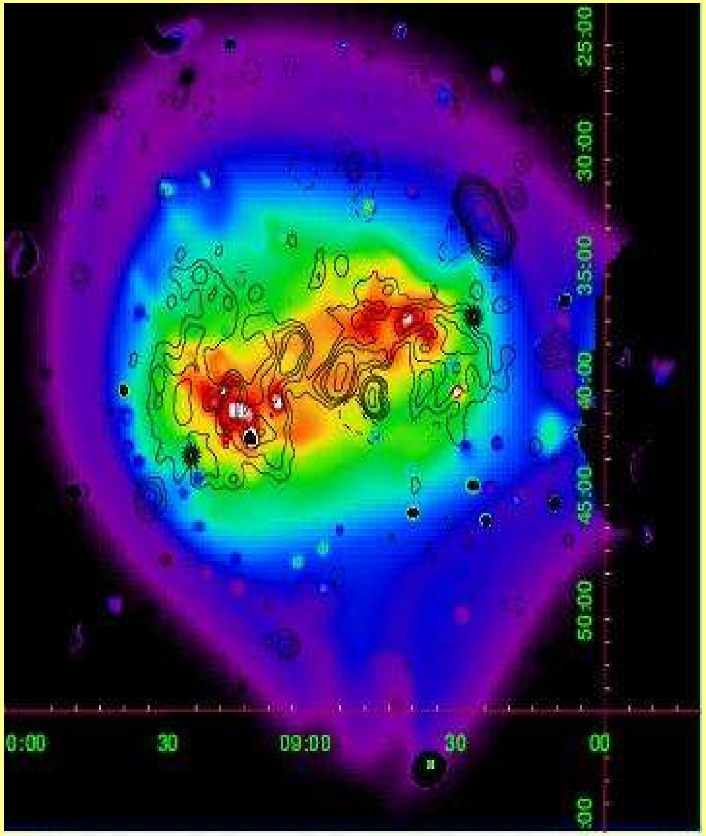

- Extended brehmsstrahlung (radio) + FE XVII (hard X) due to Intergalactic Gas in equilibrium within the Cluster potential well

Dark Matter in Clusters

Hard (> 10 keV) X-ray emission from Intergalactic Gas

Sato et al. (2000)

Total Luminosity

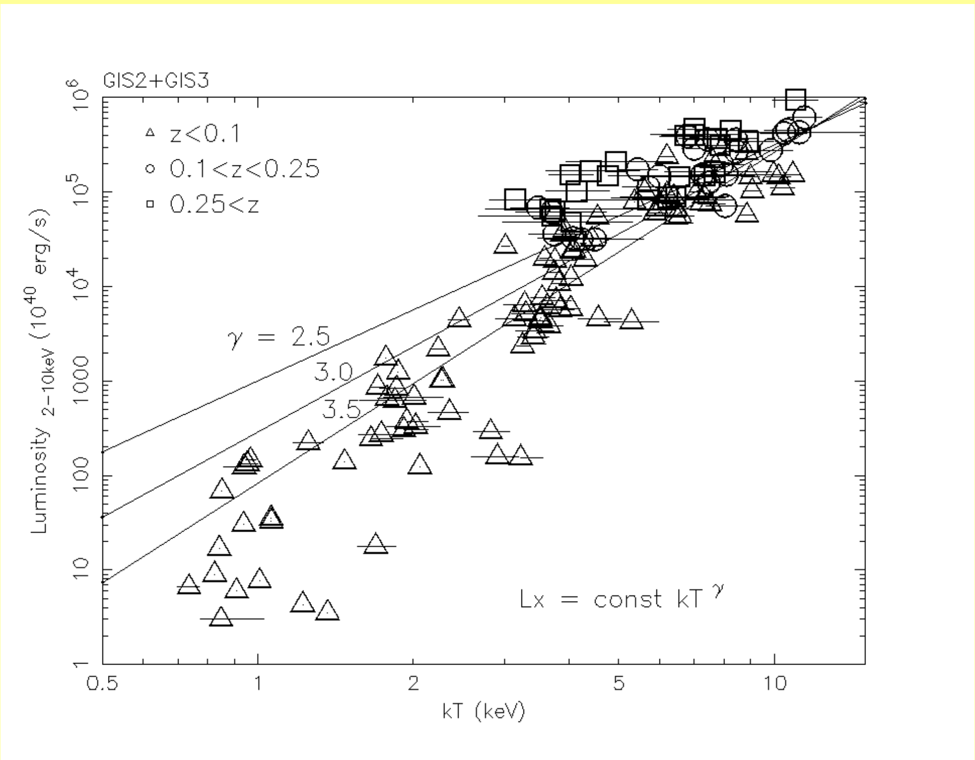

Temperature (1 kev = 1.6 10^7 K)

- T_X is a measure of M_{DM} :

Values in excess of 10^{15}-$10^{16.5}$ M_{sol} are obtained

$$\langle v \rangle^2 = \frac{2}{3}\frac{kT_x}{\mu m_H} = \frac{GM_{dyn}(R)}{R}$$

- Relation between T_X and M_{dyn} is strongly model-dependent (isothermal/power law IGM distr., spherical distr.....)

NOTE: MOND models can partially account also for Clusters (e.g. Sanders, MNRAS 342, 901 [2003])

Why Grav. Lensing is an evidence for DM?

- A *purely general relativistic effect*: its mere detection is consistent with the "Standard" Cosmological Model

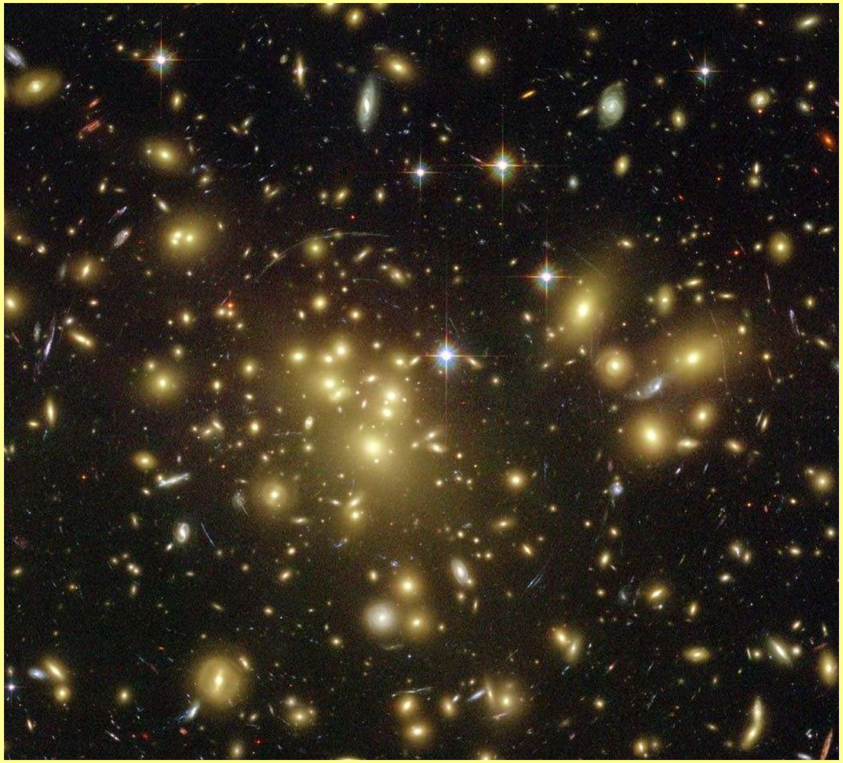

Abell 1689 (HST/NASA)

- <u>Model independent</u> / No hypothesis on IGM distr. and/or galaxies-DM relationship

- 2 main usages:

a) Determining Omega_DM, etc *cosmological WL*

b) Mass reconstruction of LSS

Clusters of galaxies, galaxy halos

What is Weak Lensing ? Does it work in practice ??

- A GR effect: Null geodesics bundles are *slightly* deformed by intervening mass-energy (*matter*)

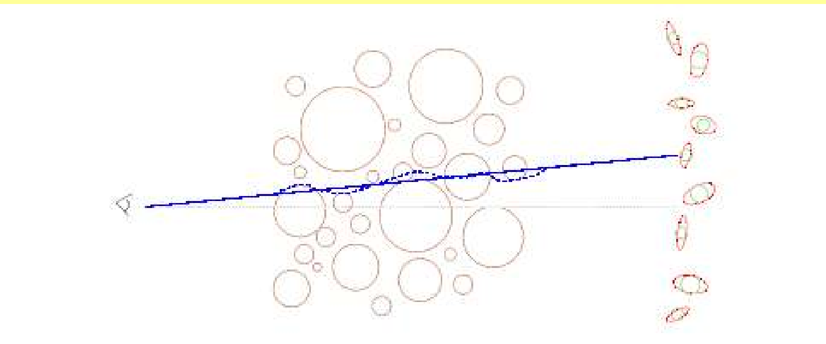

- WL regime: not quantitatively defined – practically defined when $\Delta e_1/e_1$ approx $\Delta e_2/e_2$ approx 10^{-2}

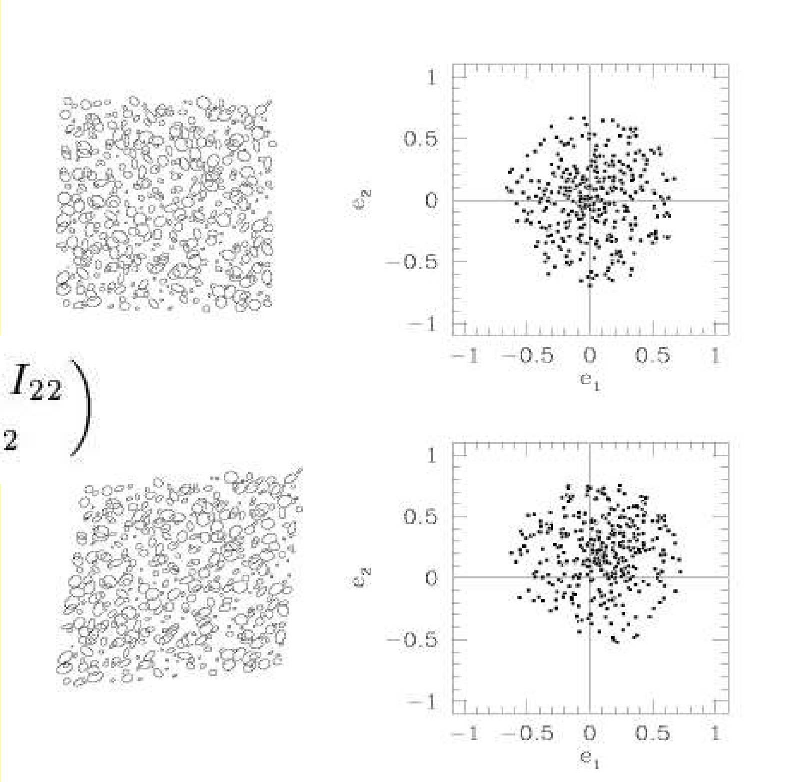

- A statistical effect: one measures (quantities connected to) *average* deviations of the ellipticities of background galaxies

$$\begin{pmatrix} e_1 \\ e_2 \end{pmatrix} = \frac{1}{I_{11} + I_{22}} \begin{pmatrix} I_{11} - I_{22} \\ 2I_{12} \end{pmatrix}$$

Main reference: Bartelmann & Schneider, Phys. Reports, 340, 291 (2001)

WL technology

- Wide *field of view* Schmidt telescopes (e.g. ESO VST@Paranal)

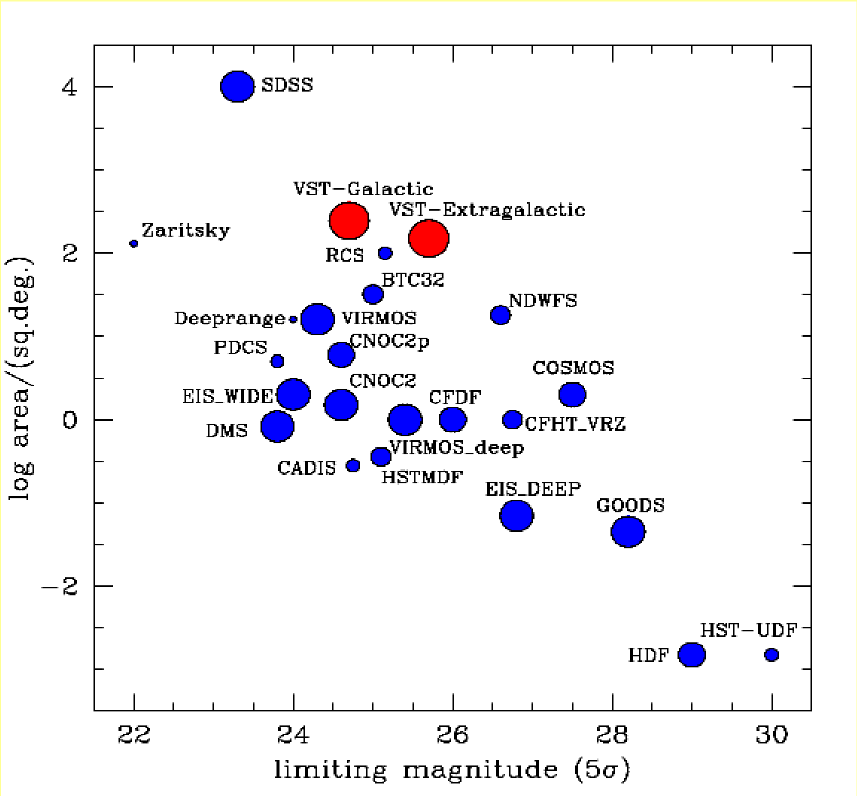

- VST-16 EG-survey: highest FOV @ R<= 25.5 -> approx. aver. 38.5 bkg. gals. arcmin^{-2} for WL purposes

WL surveys requirements

- Very high image quality + <u>very stable PSF</u>

for accurate shape measurements

- High gals. surface density (10 – 100 gals. arcmin^{-2})

to reduce intrinsic and interlopers' statistical noise

- Wide survey area (> 1-2 sq. degs.)

to reduce cosmic variance

The mere presence of signal strongly depends on a trade-off among these factors

- Systematics effects seriously threaten the signal

LSS in front and behind the cluster, telescope distortions, CCD non-unifomity

$(\Delta\gamma/\gamma) < \approx 10^{-3}$ but $(\Delta\gamma/\gamma)_{sys} \approx 10^{-2}$

The WL signal is typically extracted from noisy images

Distant (z approx 1)
bkg. gals

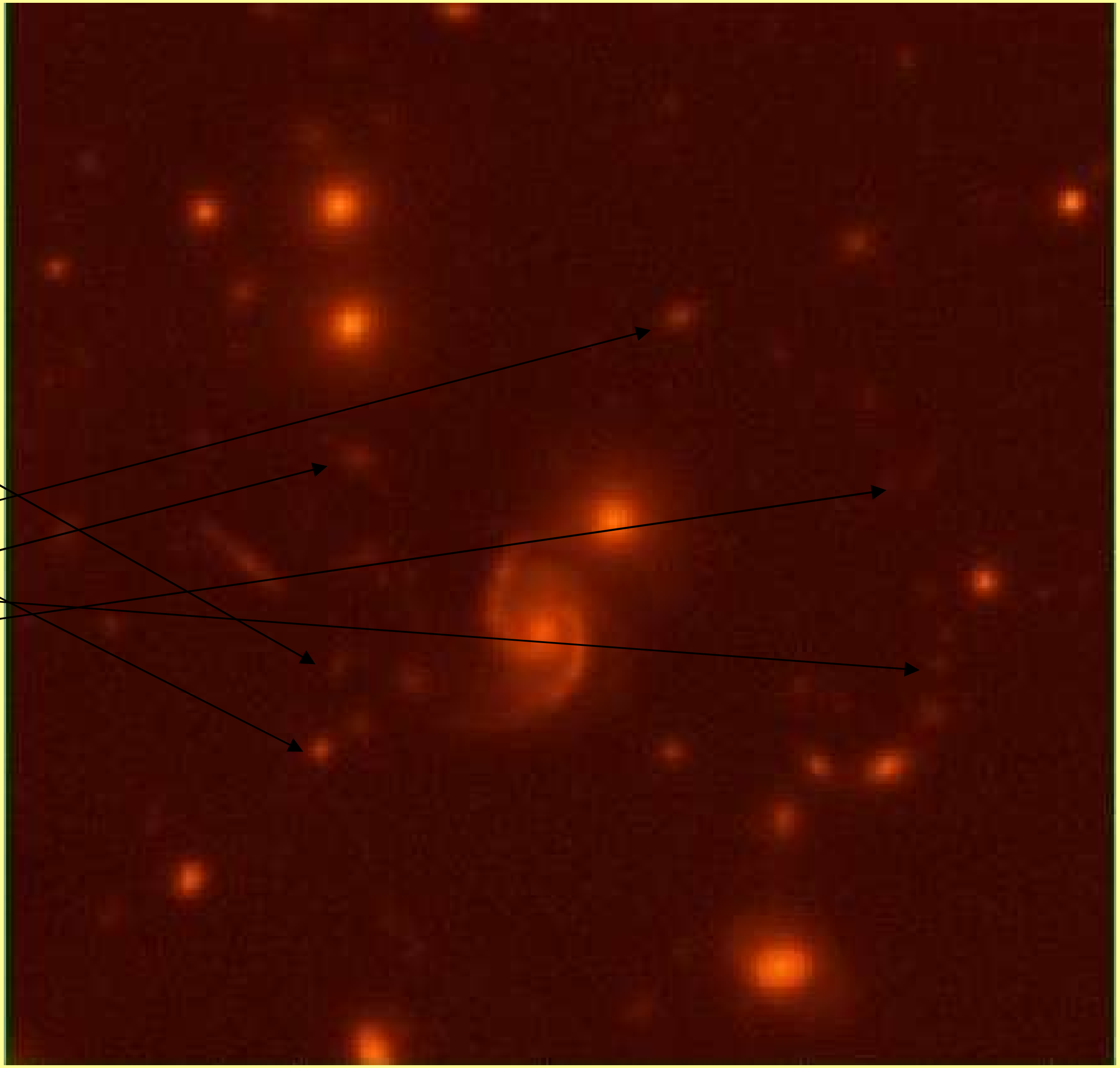

Central region of Abell 209

Geometry of Grav. lensing

- Lens equation in Born *(thin lens)* Approx. : geodesics deviation approximated as a single scattering event on the lens plane

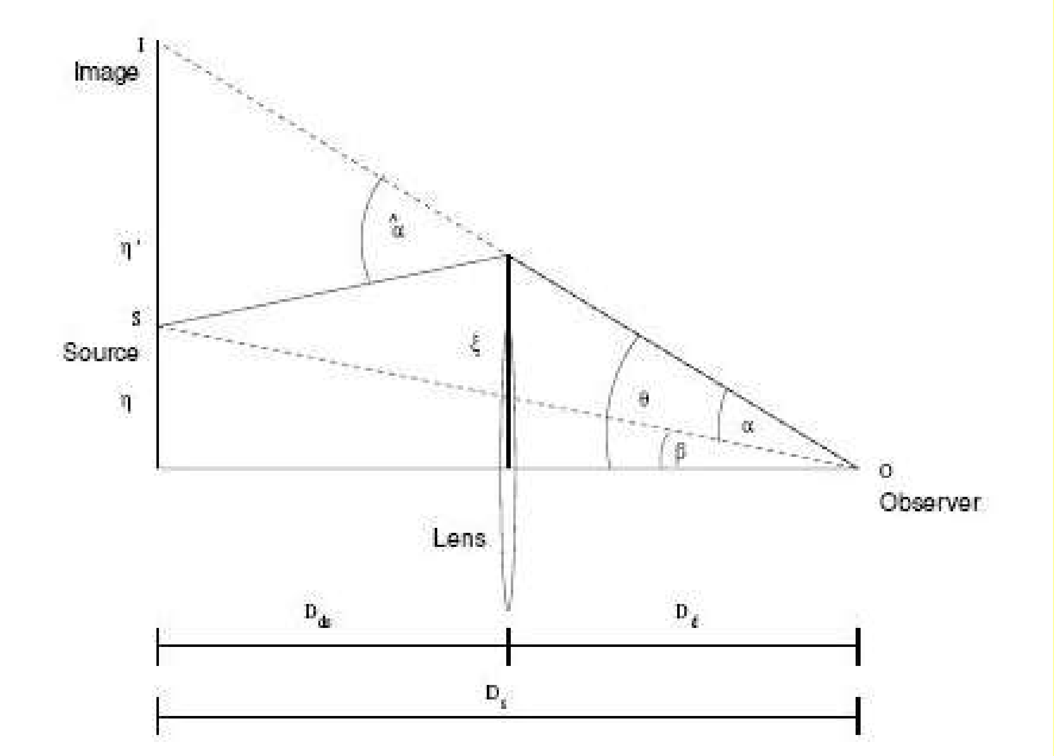

- Valid as far as beta, alpha, theta and Phi/c^2 << 1

E.g.: M approx 10^{15} M_{sol} one gets Phi approx $4.78\text{x}10^{-6}$

- From pure geometry one finds:

$$\frac{\boldsymbol{\xi}}{D_d} = \frac{\boldsymbol{\eta}'}{D_s}$$

and:

$$\boldsymbol{\eta} = \boldsymbol{\eta}' - \tilde{\boldsymbol{\alpha}} D_{ds} = \boldsymbol{\xi} \frac{D_s}{D_d} - \tilde{\boldsymbol{\alpha}} D_s$$

divide by D_s to get: $\boldsymbol{\beta} = \boldsymbol{\vartheta} - \boldsymbol{\alpha}(\boldsymbol{\vartheta})$

$$\boldsymbol{\beta} = \boldsymbol{\vartheta} - \boldsymbol{\alpha}(\boldsymbol{\vartheta})$$

- GR in 1st order (*newtonian*) approx. enters here:

$$\boldsymbol{\alpha}(\boldsymbol{\vartheta}) = \frac{1}{\pi}\int d\boldsymbol{\vartheta}'\kappa(\boldsymbol{\vartheta}')\frac{\boldsymbol{\vartheta}-\boldsymbol{\vartheta}'}{|\boldsymbol{\vartheta}-\boldsymbol{\vartheta}'|^2}$$

where one has defined:

$$\kappa(\boldsymbol{\vartheta}) = \frac{\kappa(\boldsymbol{\vartheta})}{\Sigma_{crit}}$$

$\kappa(\theta)$ is prop. to the proj. density along the l.o.s, and the *critical density*:

$$\Sigma_{crit} = \frac{c^2}{4\pi G}\frac{D_s}{D_d D_{ds}}$$

- $D_{(s,d,ds)}$ are all angular diameter cosmological distances

Measuring shape

- Quantifying deformation: 4-pole or higher moments of I(θ)

$$Q_{ij} = \frac{\int \mathrm{d}^2\theta\, q_I[I(\boldsymbol{\theta})](\theta_i - \bar{\theta}_i)(\theta_j - \bar{\theta}_j)}{\int \mathrm{d}^2\theta\, q_I[I(\boldsymbol{\theta})]}, \quad i,j \in \{1,2\}$$

- Grav. lensing modifies Q: $Q^{(s)} = \mathcal{A}\, Q\, \mathcal{A}^{\mathrm{T}} = \mathcal{A}\, Q\, \mathcal{A}\,,$ where:

$$\mathbf{A} \equiv \frac{\partial \boldsymbol{\beta}}{\partial \boldsymbol{\theta}} = \mathbf{I} - (\psi)_{ij}$$

$$\mathcal{A} = (1-\kappa)\begin{pmatrix} 1-g_1 & -g_2 \\ -g_2 & 1+g_1 \end{pmatrix}.$$

$$g(\boldsymbol{\theta}) \equiv \frac{\gamma(\boldsymbol{\theta})}{1-\kappa(\boldsymbol{\theta})}\,.$$

- γ(θ) is the deformation (*shear*)

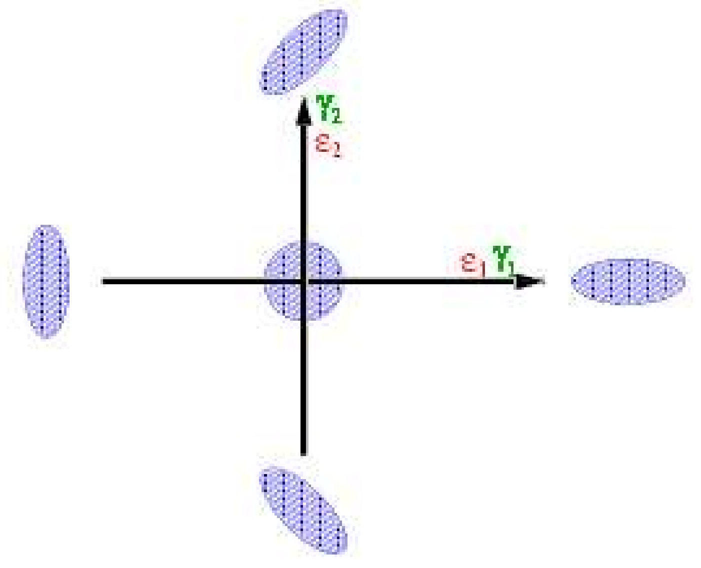

- NOTE: one actually measures Q_{ij}, i.e. $g(\theta) = \gamma(\theta)/(1 - \kappa(\theta))$

Weak Lensing regime: $\kappa(\theta) << 1$ $g(\theta)$ approx $\gamma(\theta)$

- One often works with a complex quantity:

$$\chi = \frac{Q_{11} - Q_{22} + 2\mathrm{i}Q_{12}}{Q_{11} + Q_{22}}$$

- Under WL the latter quantity transforms as:

$$\chi = \frac{\chi_{\mathrm{s}} + 2g + g^2\chi_{\mathrm{s}}^*}{1 + |g|^2 + 2\,\mathrm{Re}(g\chi_{\mathrm{s}}^*)}\,.$$

where the subscript "s" stands for "source"

The KSB+ method

Devised to correct the complex shear for PSF/seeing effects

- Detection of images: SEXTRACTOR

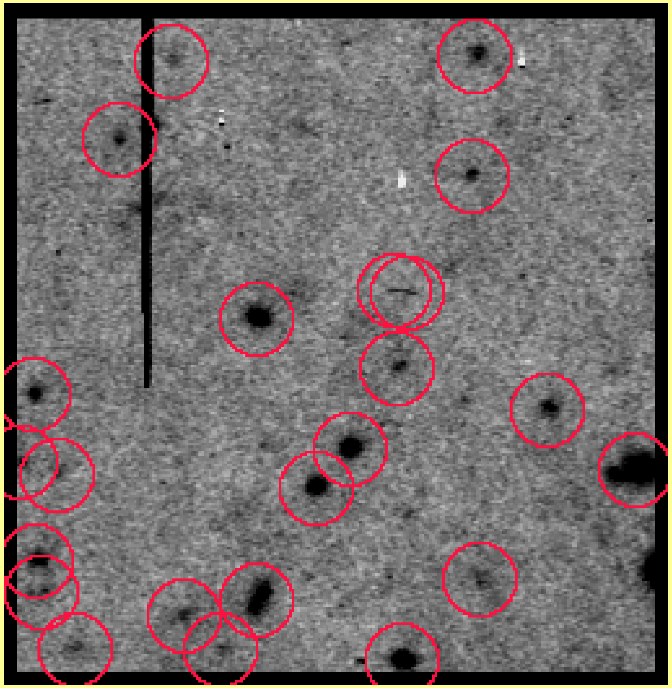

- Stars / foreground galaxies / background galaxies separation in the plans [mag-r_g] and [mag-mag(central pixel)]
- Adopt *gaussian weighted* moments to suppress bkg. noise+nearest neighbs.:

$$Q_{ij} = \int \theta_i \theta_j I(\boldsymbol{\theta}) \, W\left(\theta^2/\sigma^2\right) \, \mathrm{d}^2\theta.$$

- SPH: $\sigma = r_g$

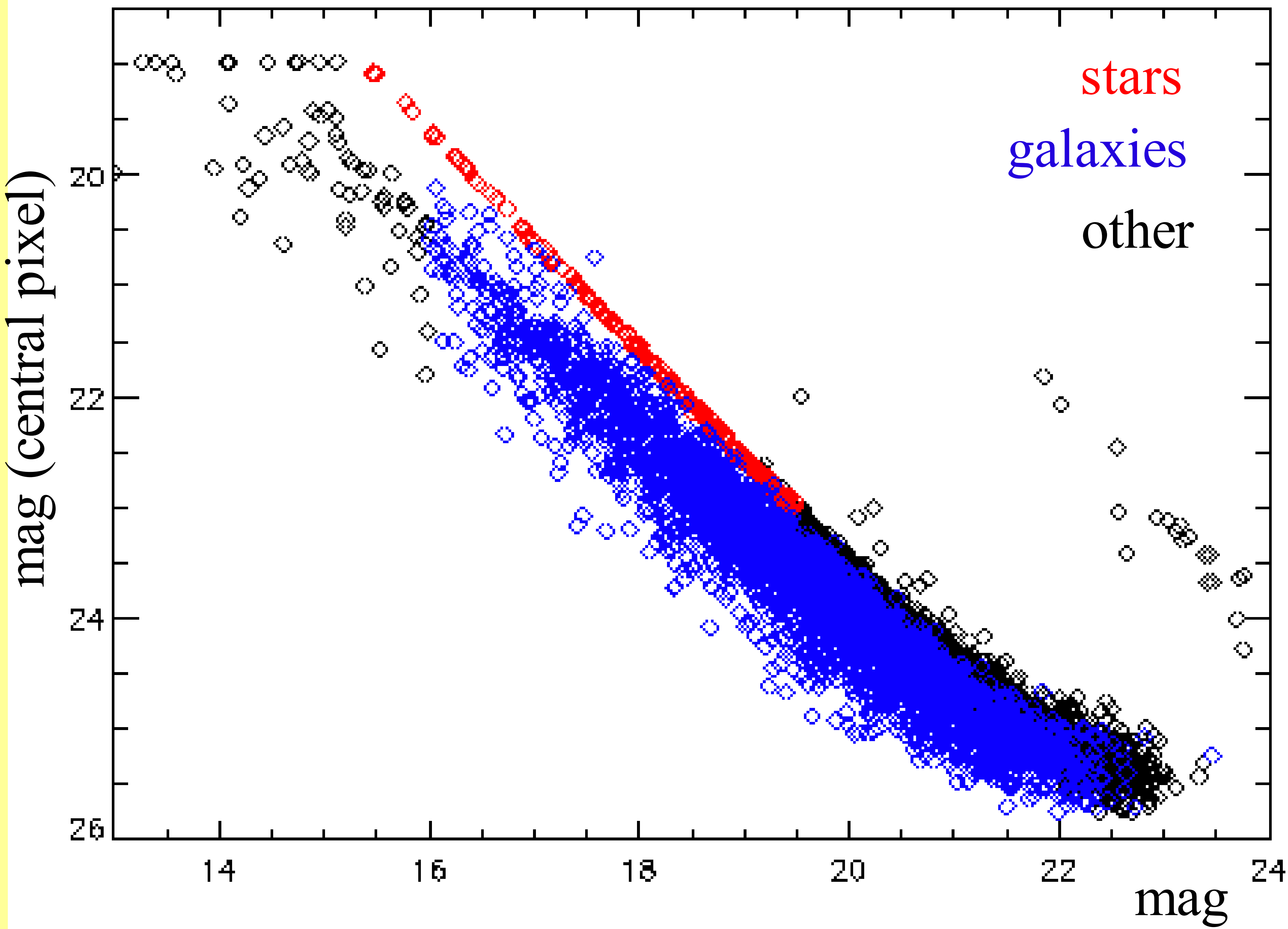
stars
galaxies
other
mag (central pixel)
20
22
24
26
14
16
18
20
22
24
mag

- Corrected shape: subtract *linear* corr. terms from PSF+atm. turb.:

$$\hat{\chi}^0_\alpha = \chi^{\rm obs}_\alpha - P^{\rm sm}_{\alpha\beta}\, q_\beta - P^{\rm g}_{\alpha\beta}\, g_\beta$$

where:

$$
\begin{aligned}
P^{\rm sm}_{\alpha\beta} &= \frac{1}{{\rm Tr}\, Q^{\rm obs}} \left(X_{\alpha\beta} - \chi^{\rm obs}_\alpha\, x_\beta\right), \\
X_{\alpha\beta} &= \int {\rm d}^2\varphi\, I^{\rm obs}(\varphi) \left[\left(W + \frac{2\varphi^2}{\sigma^2} W'\right) \delta_{\alpha\beta} + \frac{\eta_\alpha(\varphi)\eta_\beta(\varphi)}{\sigma^4} W''\right], \\
x_\alpha &= \int {\rm d}^2\varphi\, I^{\rm obs}(\varphi) \left(2W' + \frac{\varphi^2}{\sigma^2} W''\right) \frac{\eta_\alpha(\varphi)}{\sigma^2}.
\end{aligned}
$$

$(P^{\rm sm})_{\alpha\beta}$ describes the *linear response of ellipticity to PSF anisotropy*

- Smearing by *isotropic* PSF: $$\chi^{\rm iso}_\alpha = \chi^{\rm obs}_\alpha - P^{\rm sm}_{\alpha\beta}\, q_\beta$$

$q_{\beta\ \iota\sigma}$ determined by measuring the stellar anisotropy: stars are assumed to be *isotropic* and not affected by shear: $\chi_\alpha^{*,\mathrm{iso}} = 0$

implying: $q_\alpha = (P^{*,\mathrm{sm}})^{-1}_{\alpha\beta}\, \chi_\beta^{*,\mathrm{obs}}$

- $(P^g)_{\alpha\beta}$ describes the *linear correction of ellipticity to isotropic seeing:*

$$P^{\mathrm{g}}_{\alpha\beta} \;=\; C_{\alpha\beta} - P^{\mathrm{sm}}_{\alpha\gamma}(P^{*,\mathrm{sm}})^{-1}_{\gamma\delta}\, C^{*}_{\delta\beta}$$

- SPH: $(P^g)_{\alpha\beta}$ is *very noisy*, because it is evaluated at * and interpolated at different points

The KSB+ pipeline at the OACt

S. Paulin-Henriksson

- PSF correction : 6 independent polynomial fits of q_i and of $\left[\left(P_*^{sm}\right)^{-1} \cdot P_*^{sh}\right]_{i,j}$
- Tested on STEP1 ==> comparable to other KSB+ pipelines

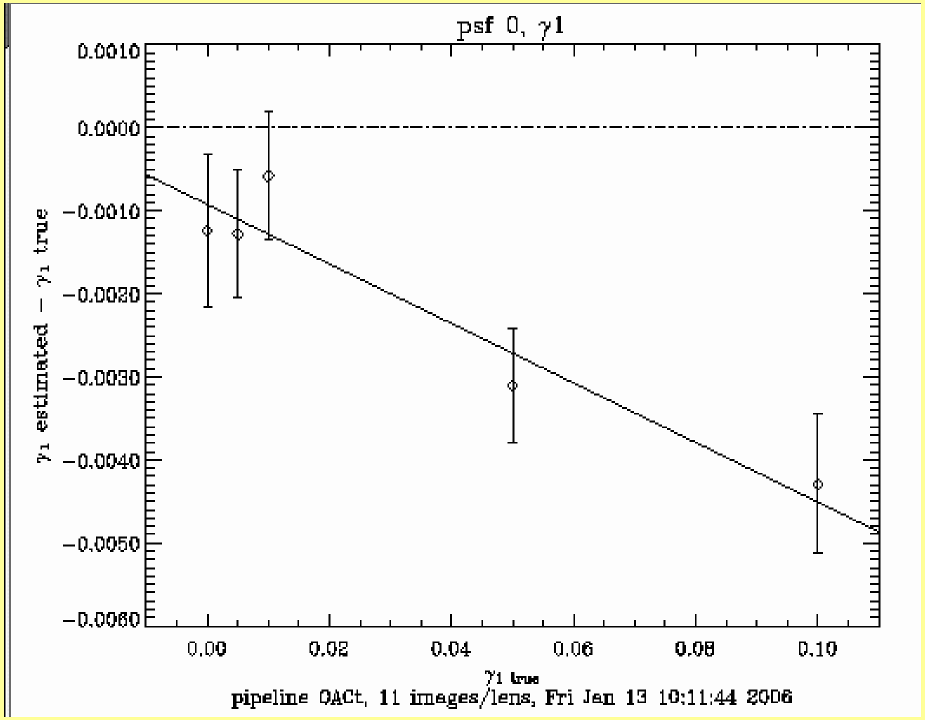

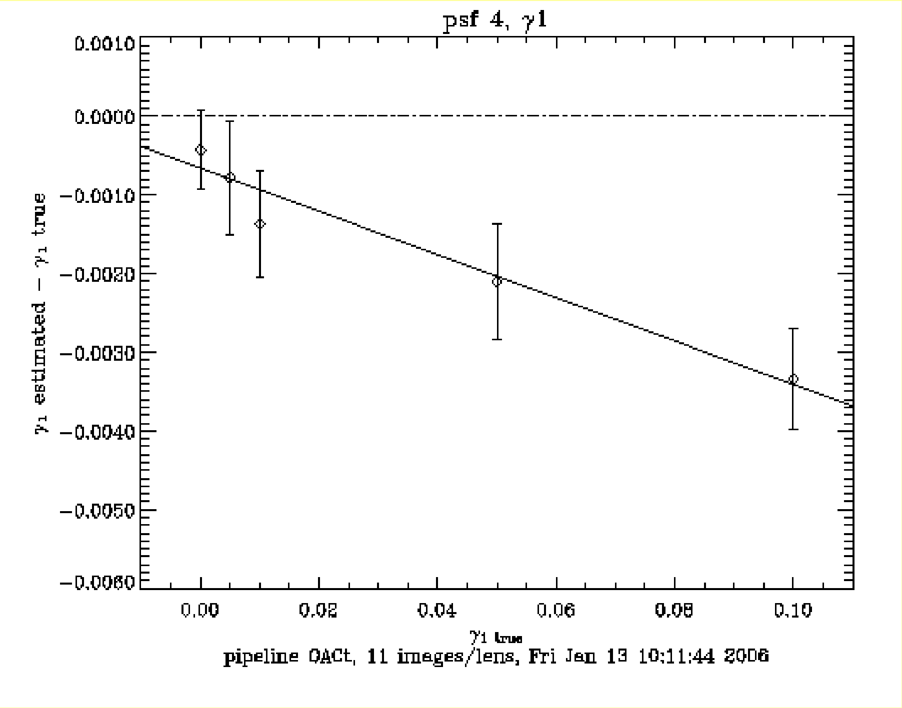

- Bias: linear dependence of shear deviation on shear

Check of the KSB+ method: STEP1 analysis

STEP1 data ==> simulation using SkyMaker,
with:

- a typical population of galaxies and stars
- sheared with a given shear constant over an image
- added on a gaussian background
- convolved with a given PSF

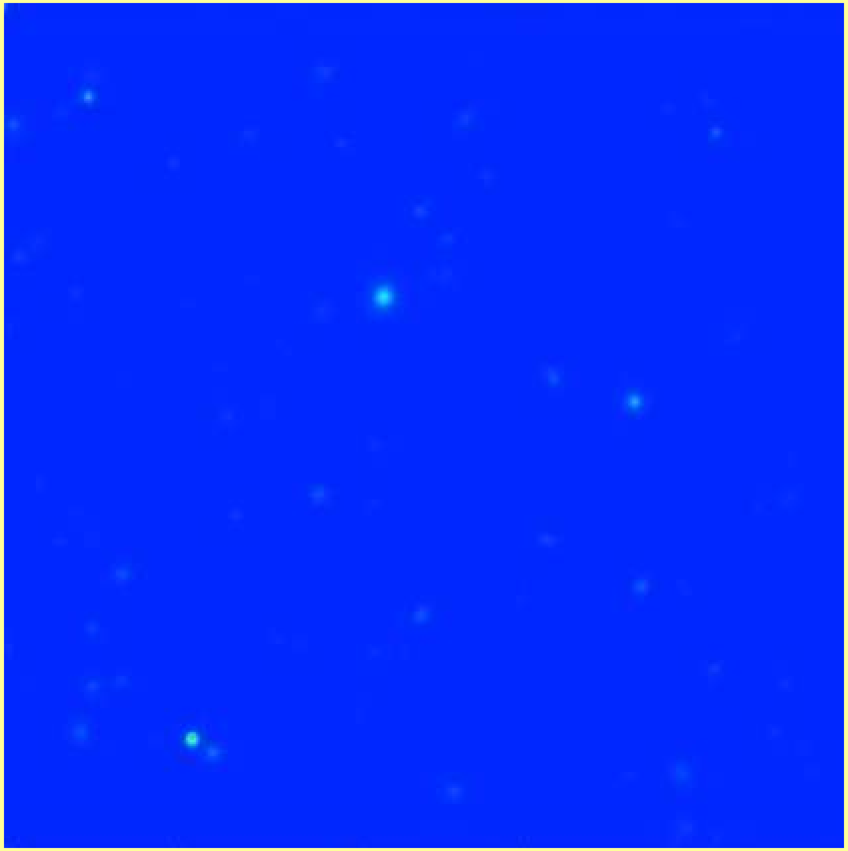

3000 galaxies x 64 images x 5 lenses x 6 PSF

KSB+ pipelines ==> small bias remaining (few %, depending on the PSF) intrinsic to the method (which is a first order correction).

- Result can strongly depend on the PSF anisotropy (verified in all STEP1 pipelines)

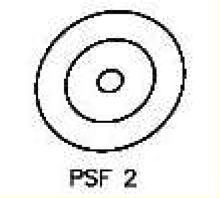

0.03/peak

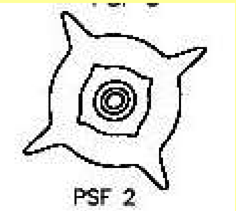

0.25/peak

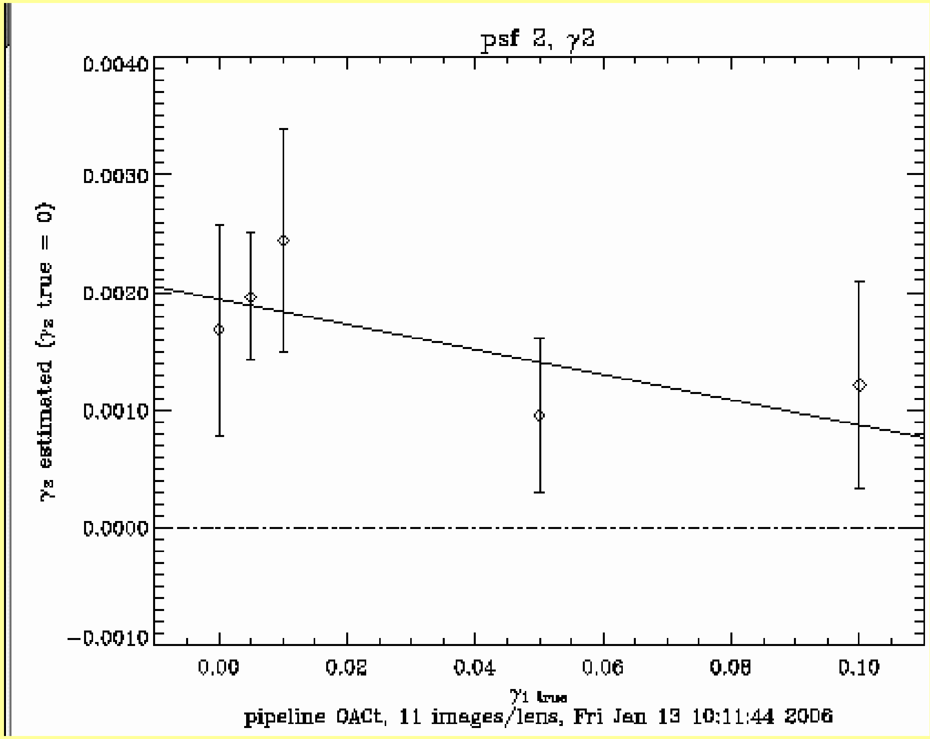

linear bias

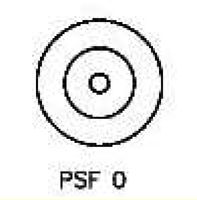

0.03/peak

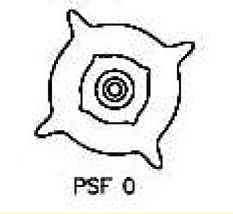

0.25/peak

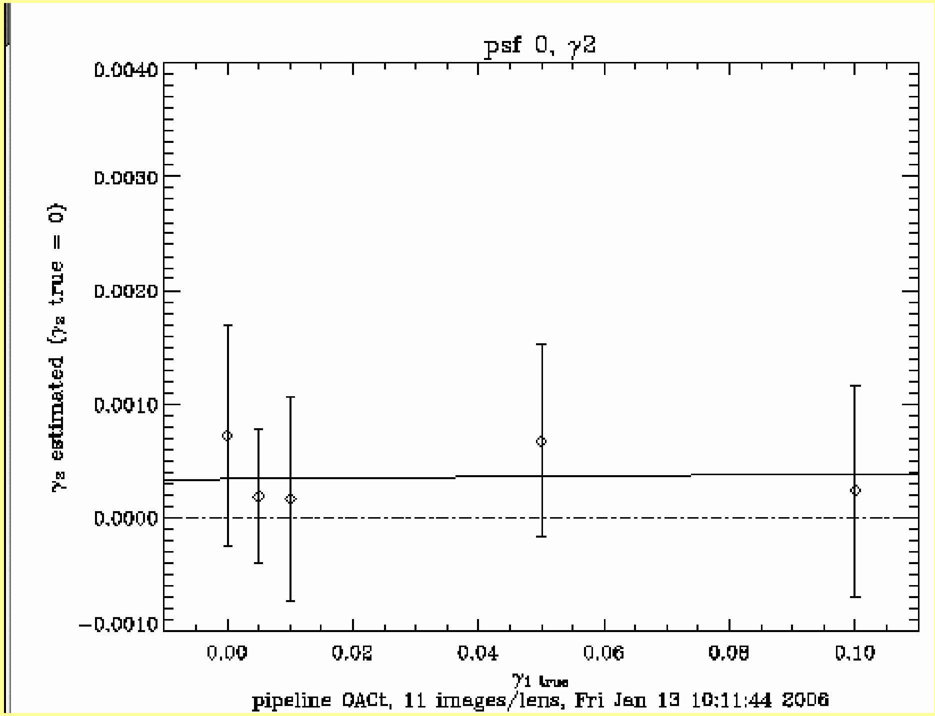

constant bias

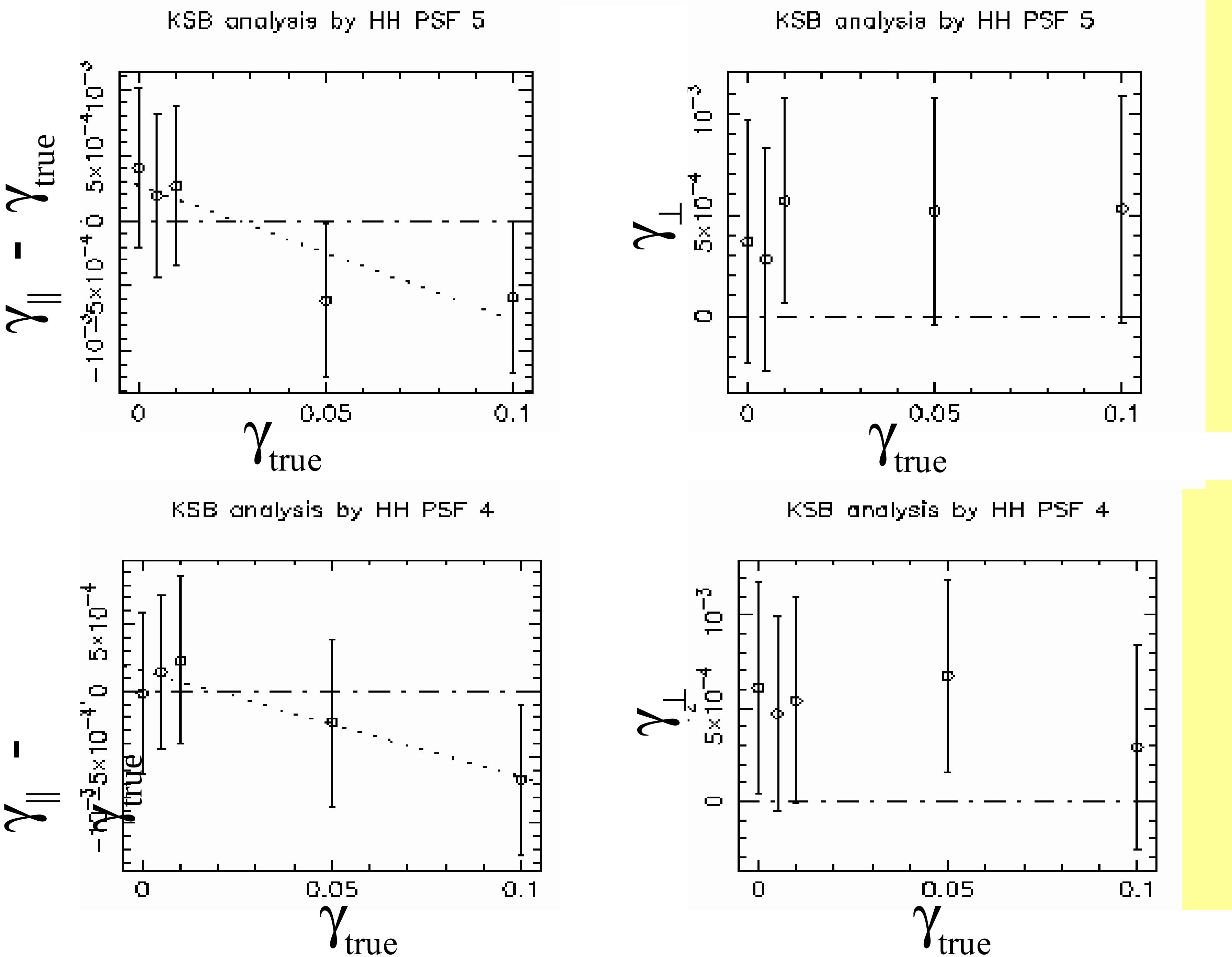
KSB analysis by HH PSF 5
KSB analysis by HH PSF 5
KSB analysis by HH PSF 4
KSB analysis by HH PSF 4
γ|| - γtrue
γ⊥
γtrue
0
0.05
0.1
−10−3
−5×10−4
5×10−4
10−3

Abell 209/CFHT12k/R-band image

R mag (central pixel)

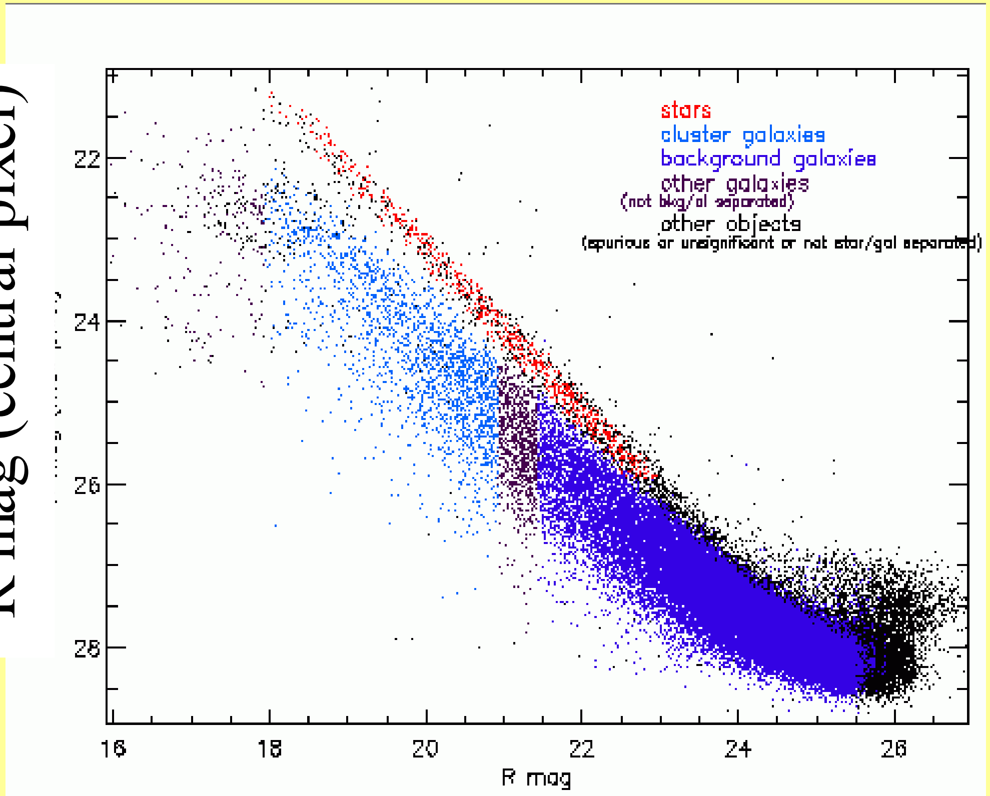

R mag

stars

cluster galaxies

background galaxies

other - other

R mag

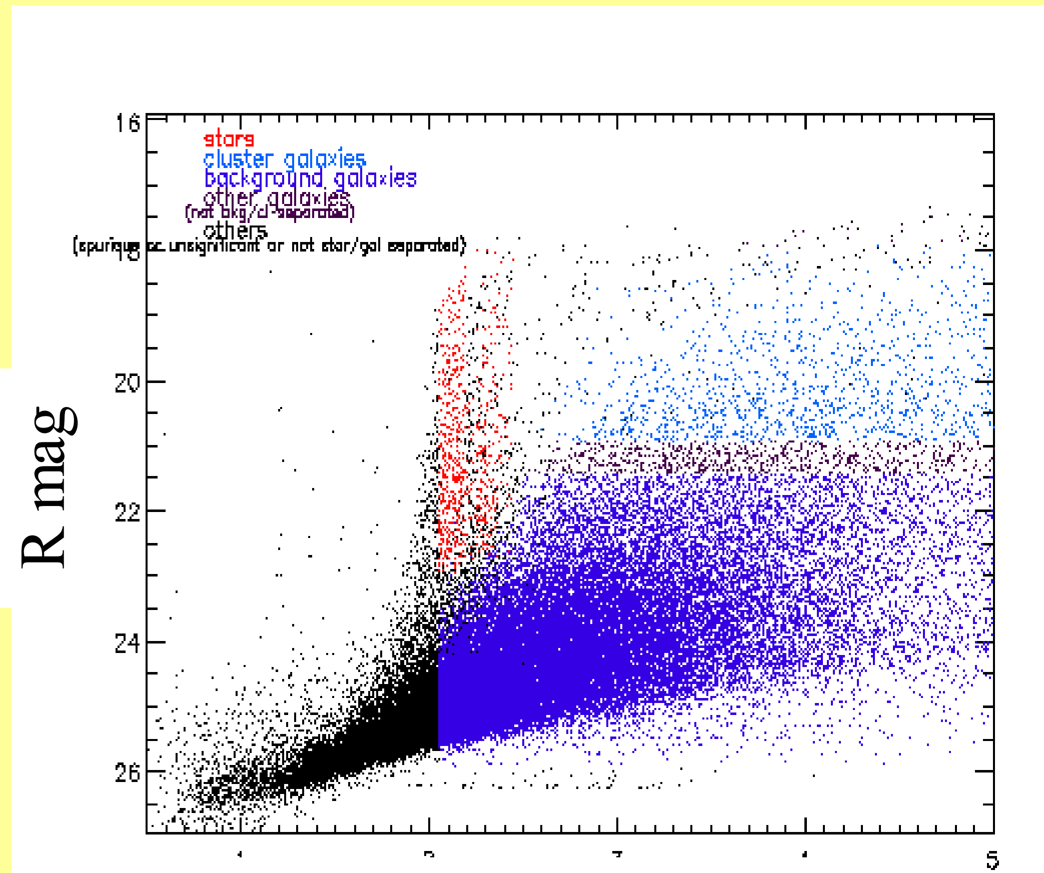

rg (sextractor flux_radius) in pixels

Abell 209 – CHFT12k - R

star ellipticity map

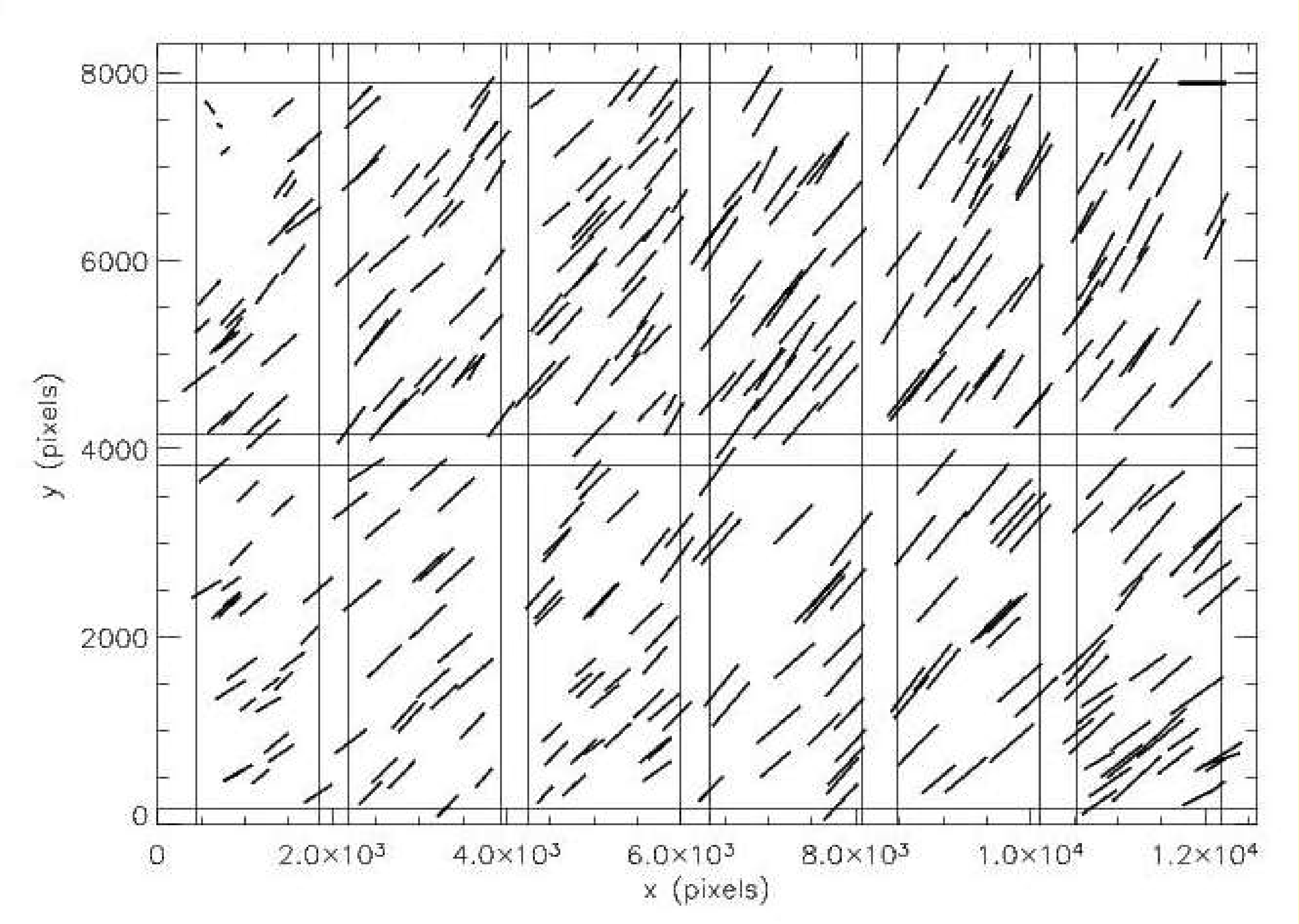

$\varepsilon = 0.08$

- WFI: 6x2 CCDs, 0.206"/pixel
- Eliminated objects lying at the border of the fields

Abell 209 – CHFT12k - R

PSF ellipticity map

$\varepsilon = 0.05$

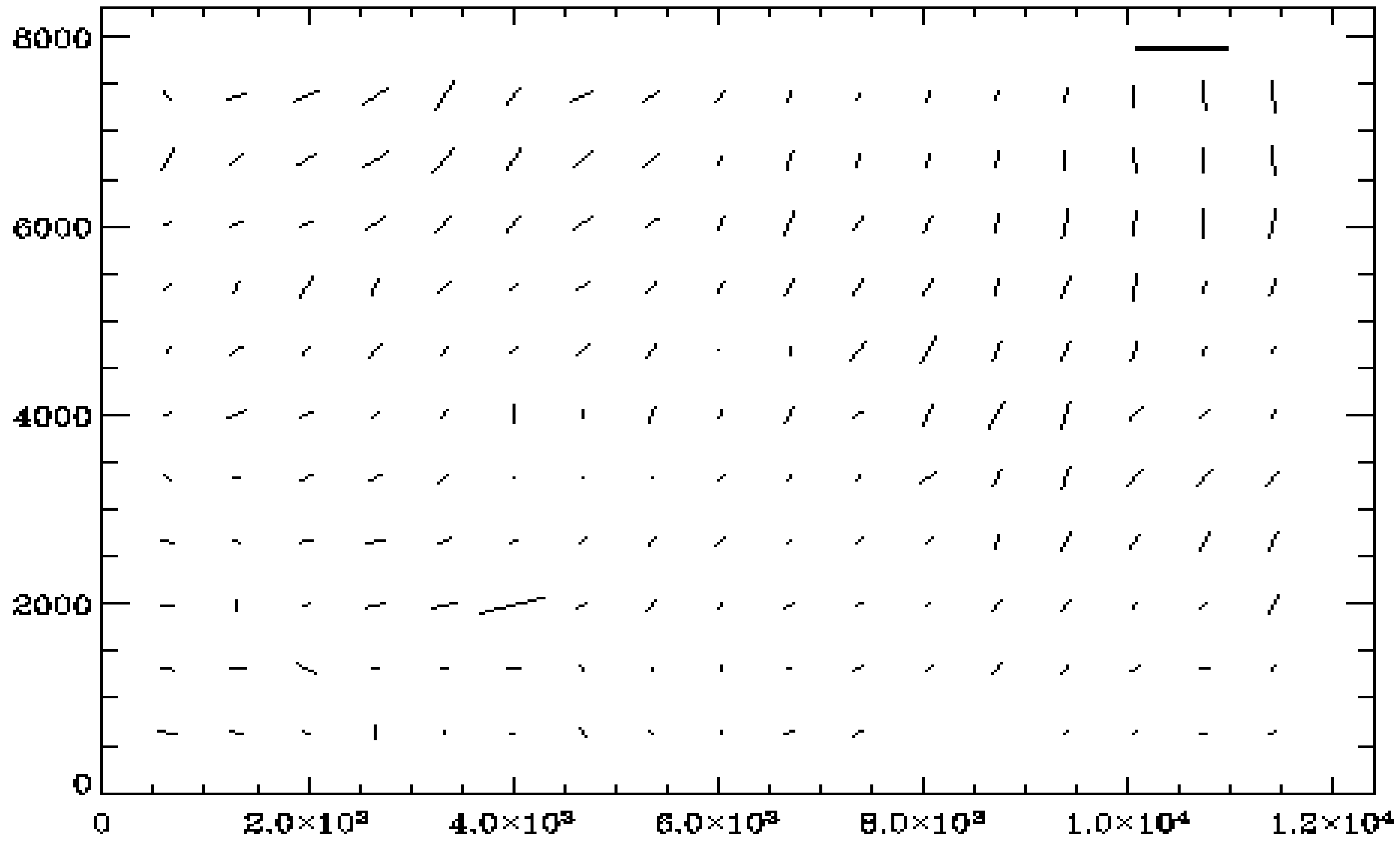

Mass Aperture statistics

- The *shear map* is still affected by *discreteness noise* -> better to look at *smoothed* maps
- Mass Aperture statistics (*Schneider & Seitz, 1995*):

$$M_{ap} \doteq \int d^2\boldsymbol{\vartheta} U(|\boldsymbol{\vartheta}|)\kappa(\boldsymbol{\vartheta})$$

Useful quantities:

$$Q(\vartheta) = \frac{2}{\vartheta^2}\int_0^{\vartheta} d\vartheta'\vartheta' U(\vartheta') - U(\vartheta)$$

$$U(\vartheta) = \frac{u(\vartheta/\theta)}{\vartheta^2}, \quad u(x) = \frac{9}{\pi}\left(1-x^2\right)\left(\frac{1}{3}-x^2\right)$$

- Using a *compensated filter*:

$$\int_0^\theta d\vartheta \vartheta U(\vartheta) = 0$$

one gets an estimator for M_{ap}:

$$m(x_0) = \int d^2y \, \gamma_t(y; x_0) \, Q(|y|).$$

i.e. directly related to the shear

- The *signal to noise* is given by:

$$S(x_0) = \frac{\sqrt{2}}{\sigma_\epsilon} \frac{\sum_i \epsilon_{ti}(x_0) Q(|x_i - x_0|)}{\sqrt{\sum_i Q^2(|x_i - x_0|)}}.$$

where:

$$\epsilon_{ti}(x_0) = -\mathcal{R}e\left(\frac{\epsilon_i (X_i - X_0)^*}{(X_i - X_0)}\right),$$

- We take: $\sigma_\varepsilon = 0.2$

A209: M_{ap} isocontours/ Dark Matter surface density profile

- Smoothing radius $R_{ap} = 4.5'$
- Slightly dependent on $U(\theta)$ More affected by R_{ap}

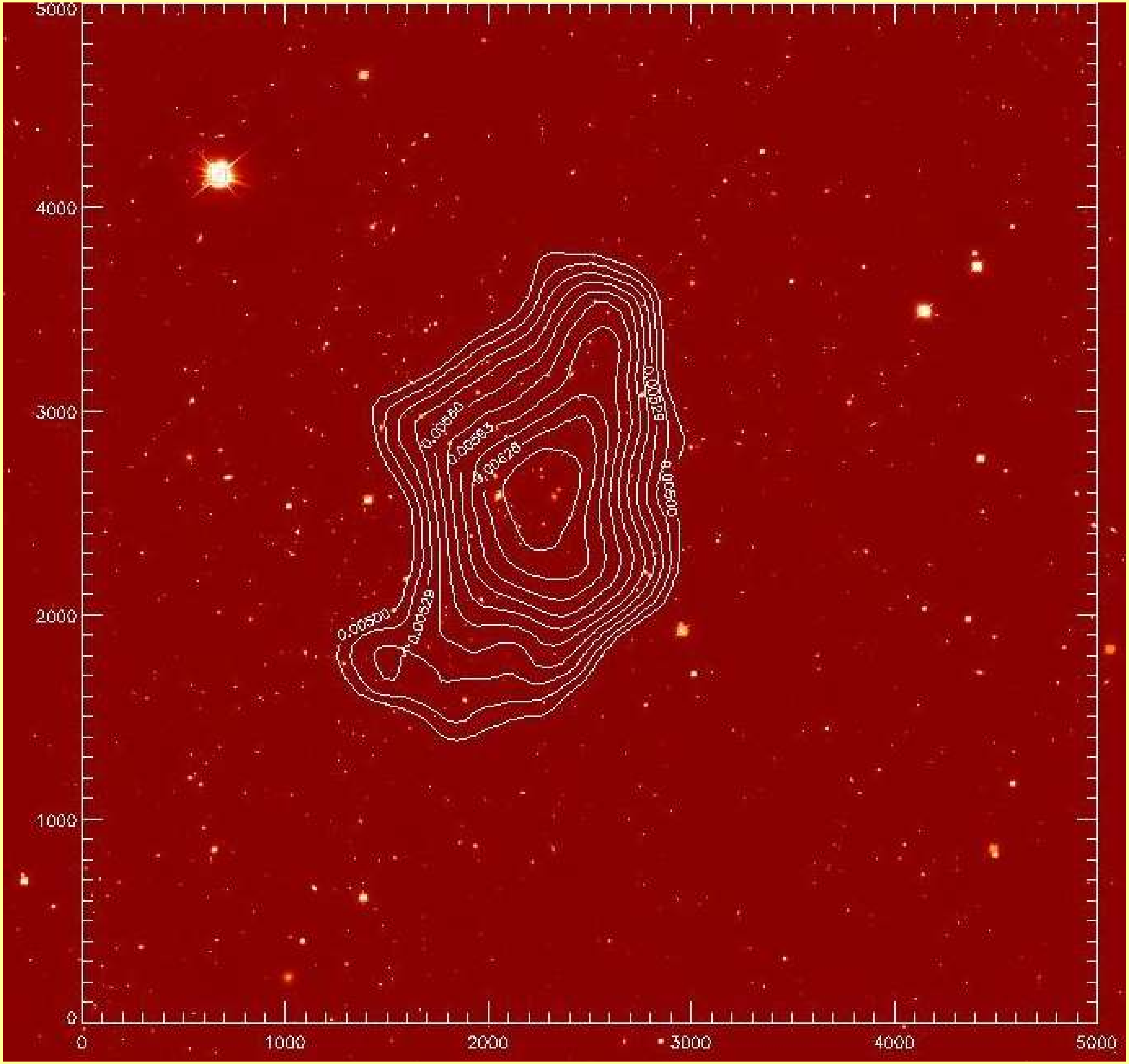

- How does it compare with Hot IGM distribution?

A 209 Chandra/ACIS 1 keV channel/ ongoing analysis by A. Pagliaro

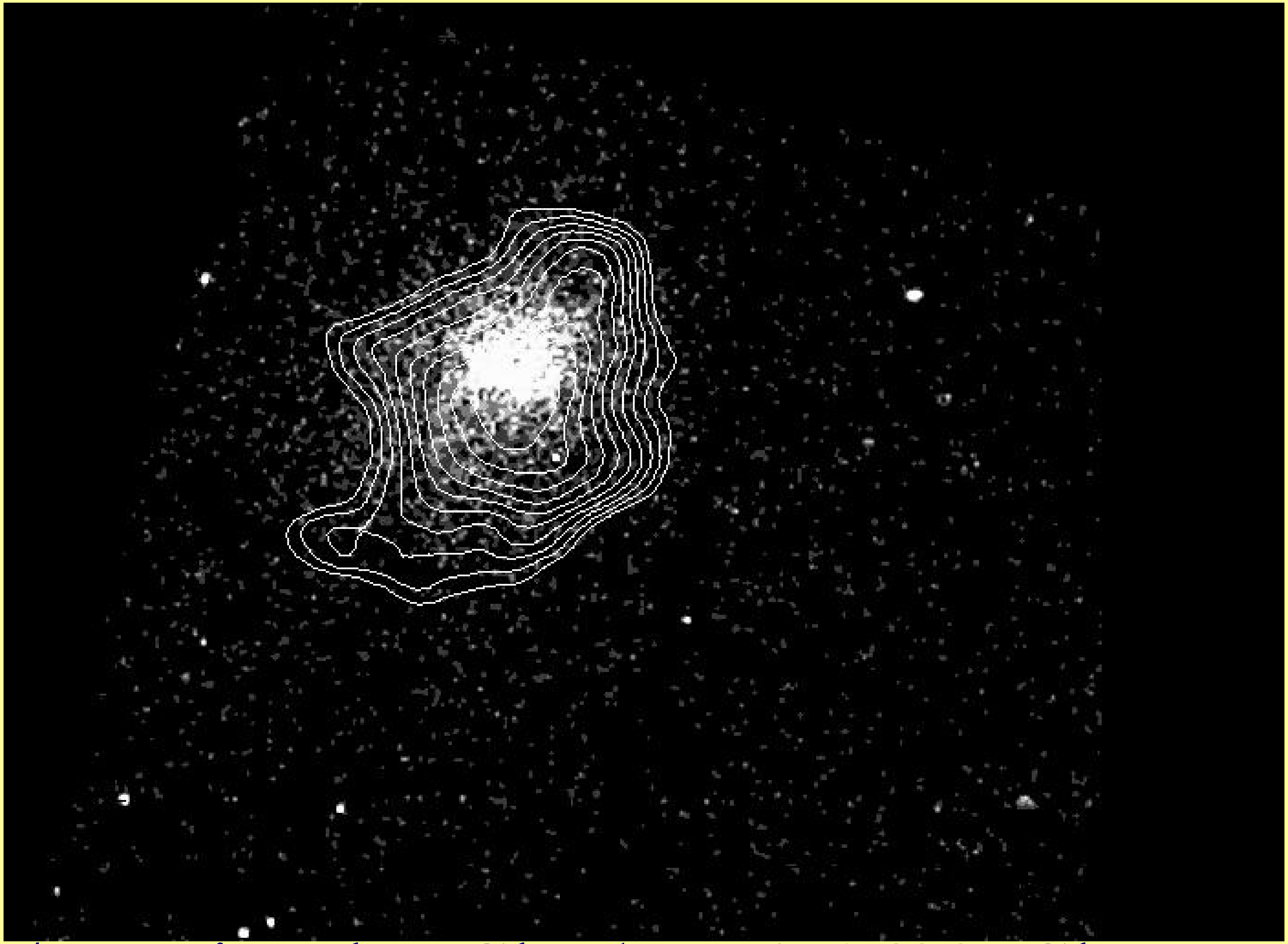

- Slightly offset / seen in other Cls. (e.g. A 1689, Clowe et al., 2001)

Abell 209
galaxy density
in R band
+
aperture mass
isocontours

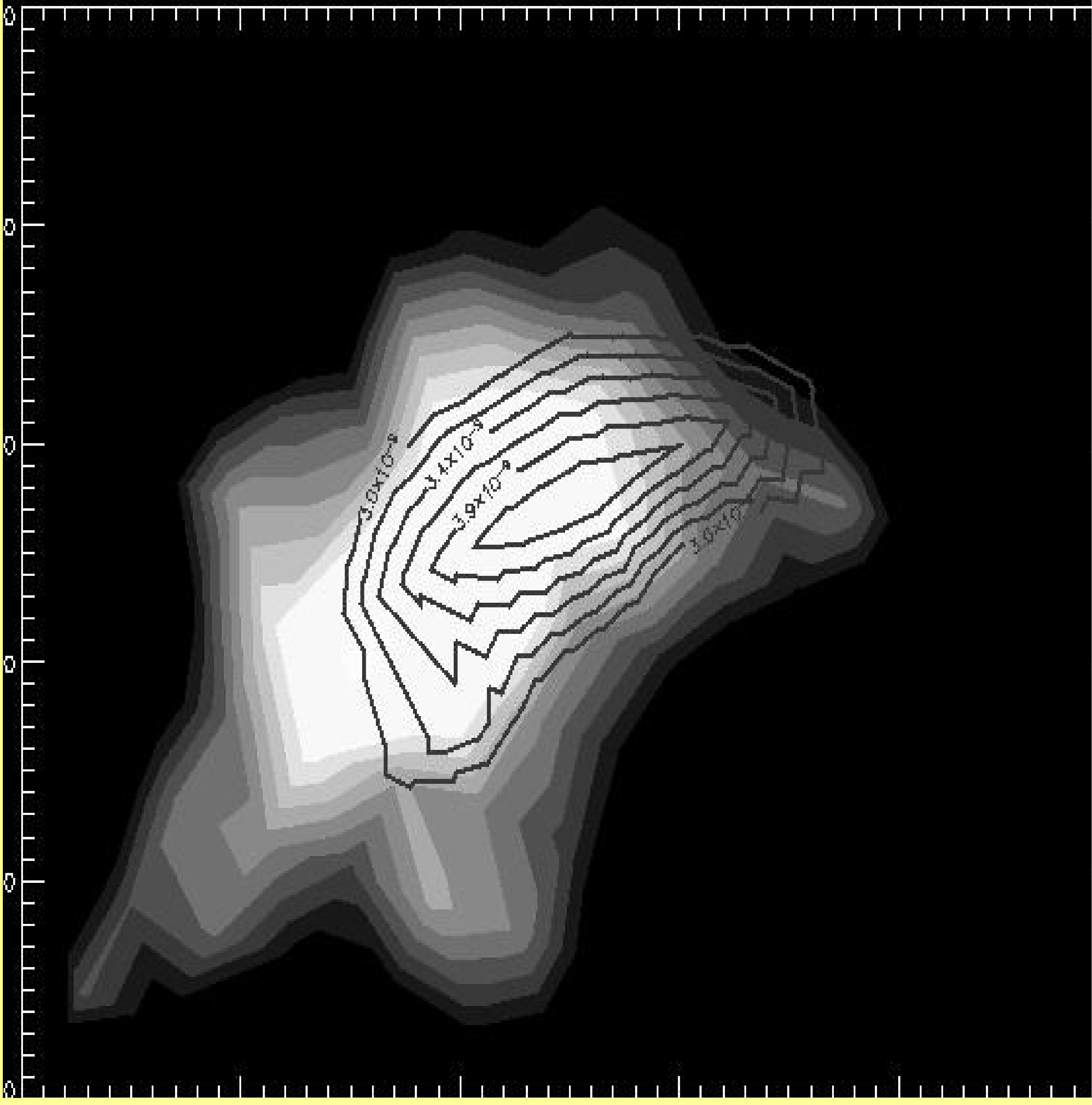

Internal consistency check

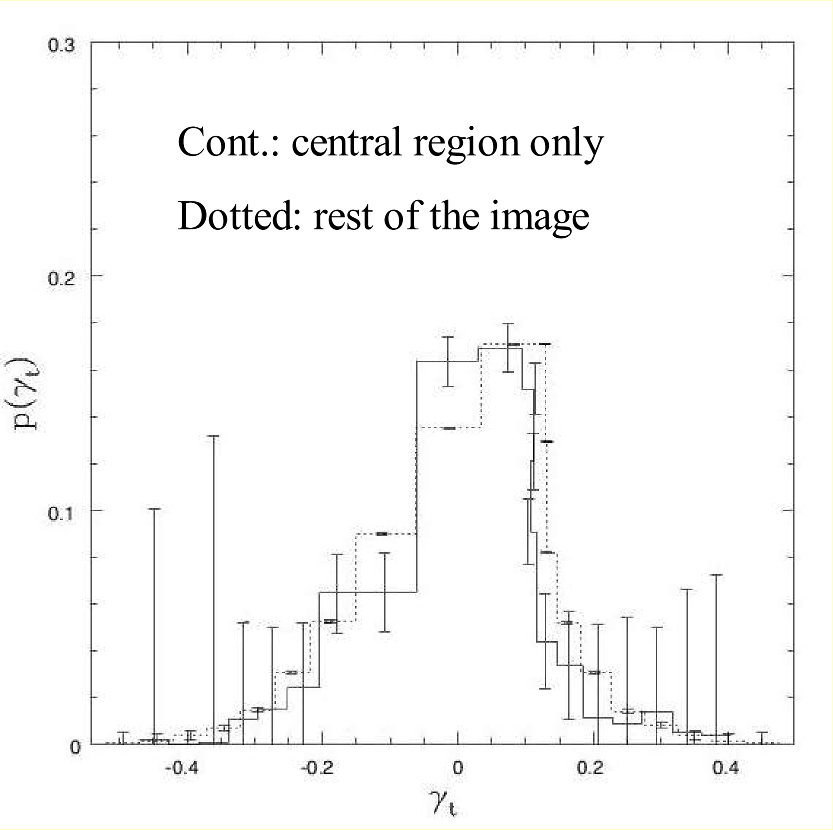

Shear prob. distribution – all

Error bars: Poisson noise

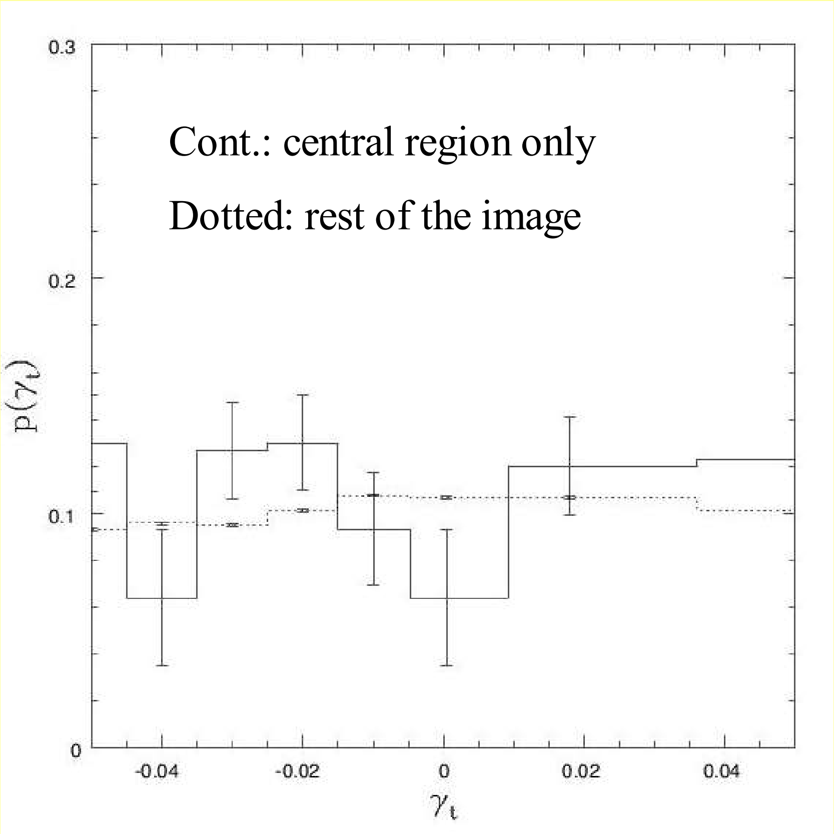

Shear prob. distribution - central isod. contours only

KS: 99.99% different distrs.

- For $|\gamma_t| < 4\mathrm{x}10^{-2}$ the distrs. are different -> WL

Mass Reconstruction: Parametric

- Beyond Mass Aperture: direct reconstruction of the density profile
- 2 approaches: Parametric and Mass Reconstruction

Parametric: Fitting a NFW or Isothermal spher. aver. profile

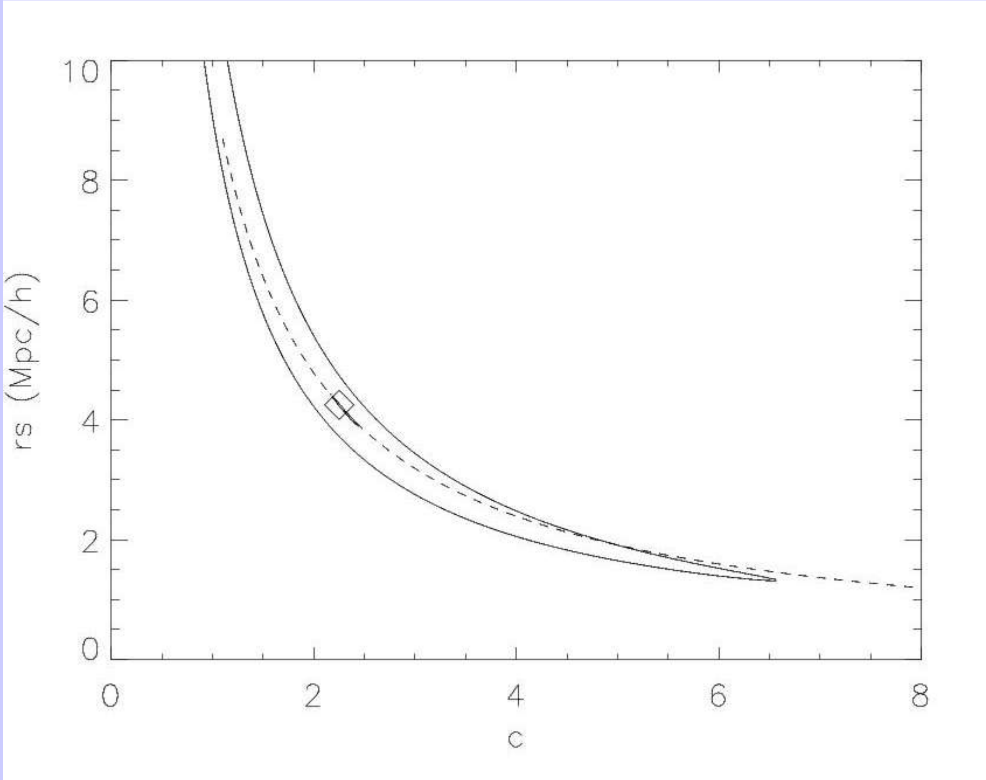

- 99.9% CL, rs = 4.5', c = 2.15 -> $r_{200} = cr_s = 2.014\ h^{-1}$ Mpc, $M_{200} = 1.881 \times 10^{15}\ M_{sun}$
- M(< 500 kpc) = $9.26 \pm 0.5 \times 10^{14}\ M_{sun}$, larger than Smith et al. (2005) for the same cluster (1.6×10^{14} Msun).

- Radovich: independent analysis, KSB+ pipeline form T. Erben

$$M_{200} = 1.05 \times 10^{15} \; (+ 4.35 \; / \; -3.05 \;\; 10^{14}) \; M_{sun}$$

$r_{200} = 1.7\ h^{-1}$ Mpc, $c = 2.10$

SIS fit: $\sigma_V = 810.39\ (+57.61\ /\ -62.39)$ Km/sec

Mass Reconstruction: Direct Inversion

- Schneider (1995) $\nabla K = \mathbf{u}(\boldsymbol{\theta})$ where: $K(\boldsymbol{\theta}) = \ln\left[1 - \kappa(\boldsymbol{\theta})\right]$

$$\mathbf{u}(\boldsymbol{\theta}) \equiv -\frac{1}{1-\mid g \mid^2}\begin{pmatrix} 1-g_1 & -g_2 \\ -g_2 & 1+g_1 \end{pmatrix}\begin{pmatrix} g_{1,1}+g_{2,2} \\ g_{2,1}-g_{1,2} \end{pmatrix}$$

and: $\mathbf{g} \div \frac{\gamma}{1-\boldsymbol{\kappa}} \approx \gamma$

- Schneider & Seitz (2001): an elliptic problem is numerically more stable

Take divergence of the first eqn.: $\nabla^2 K = \nabla \cdot \mathbf{u}$

Solve the Neumann problem: $\mathbf{n} \cdot \nabla K \mid_{\mathcal{B}} = \mathbf{n} \cdot \mathbf{u} \mid_{\mathcal{B}}$

Problem: consistent sols. of the Neumann problem must have the line integral of the normal der. along the boundary = 0

→This amounts to impose an arbitrary zero point (*mass-sheet degeneracy*)

- We prefer to solve the Dirichlet (boundary value) problem, fixing at the beginning the b.c. so that (e.g.) the mass M_{200} is the same as for the NFW fit
- Instead of SOR (single mesh) we adopt a Galerkin Hierarchical Adaptive Multigrid solver (MGGHAT, Mitchell [1997])

- div·u over the central region of A209

- 2 deep minima -> sources of K
- NOTE: south is up, and left-> right counterclockwise

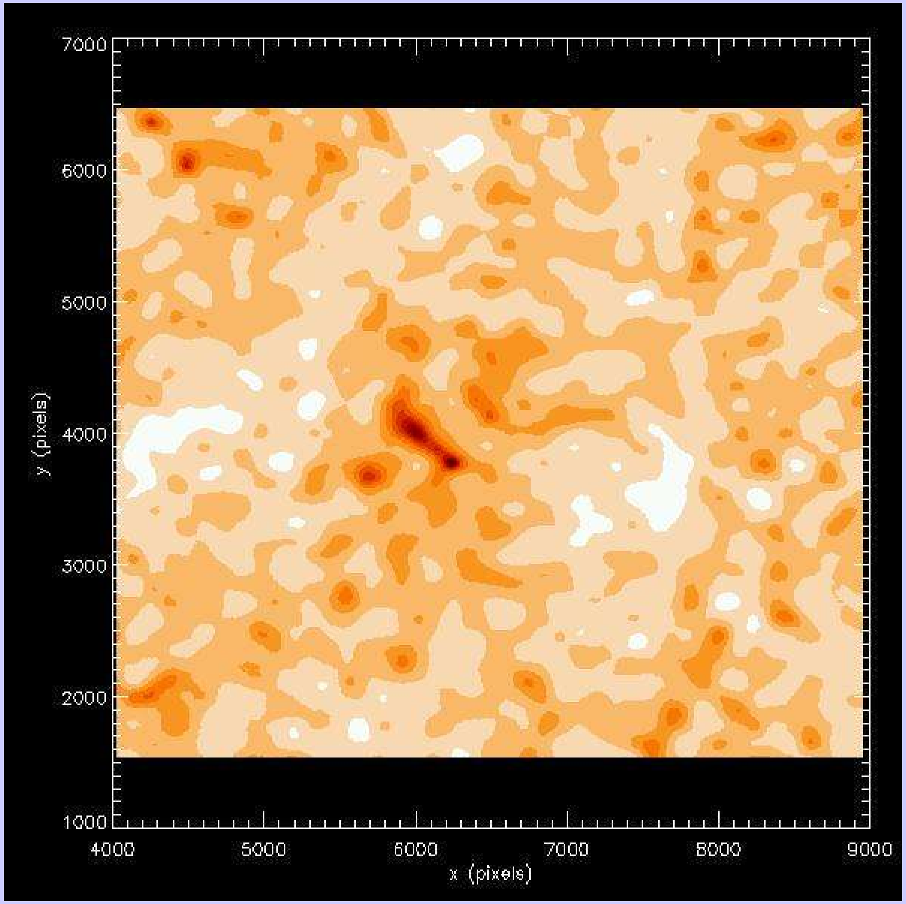

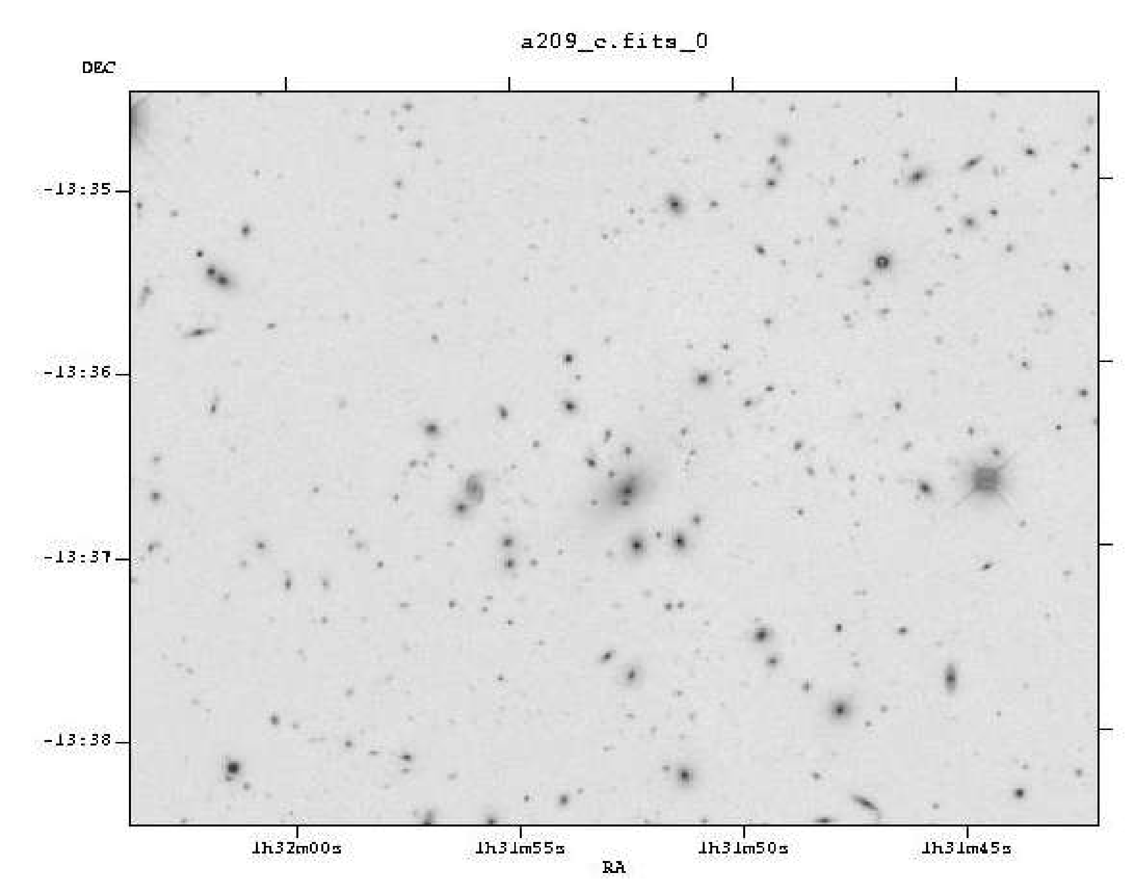

Final Mass reconstructed profile

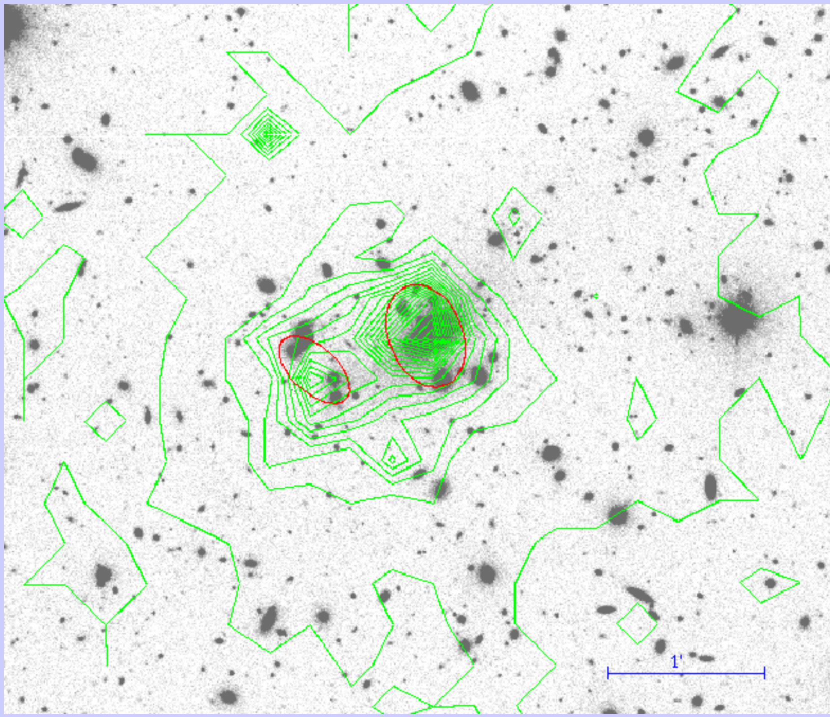

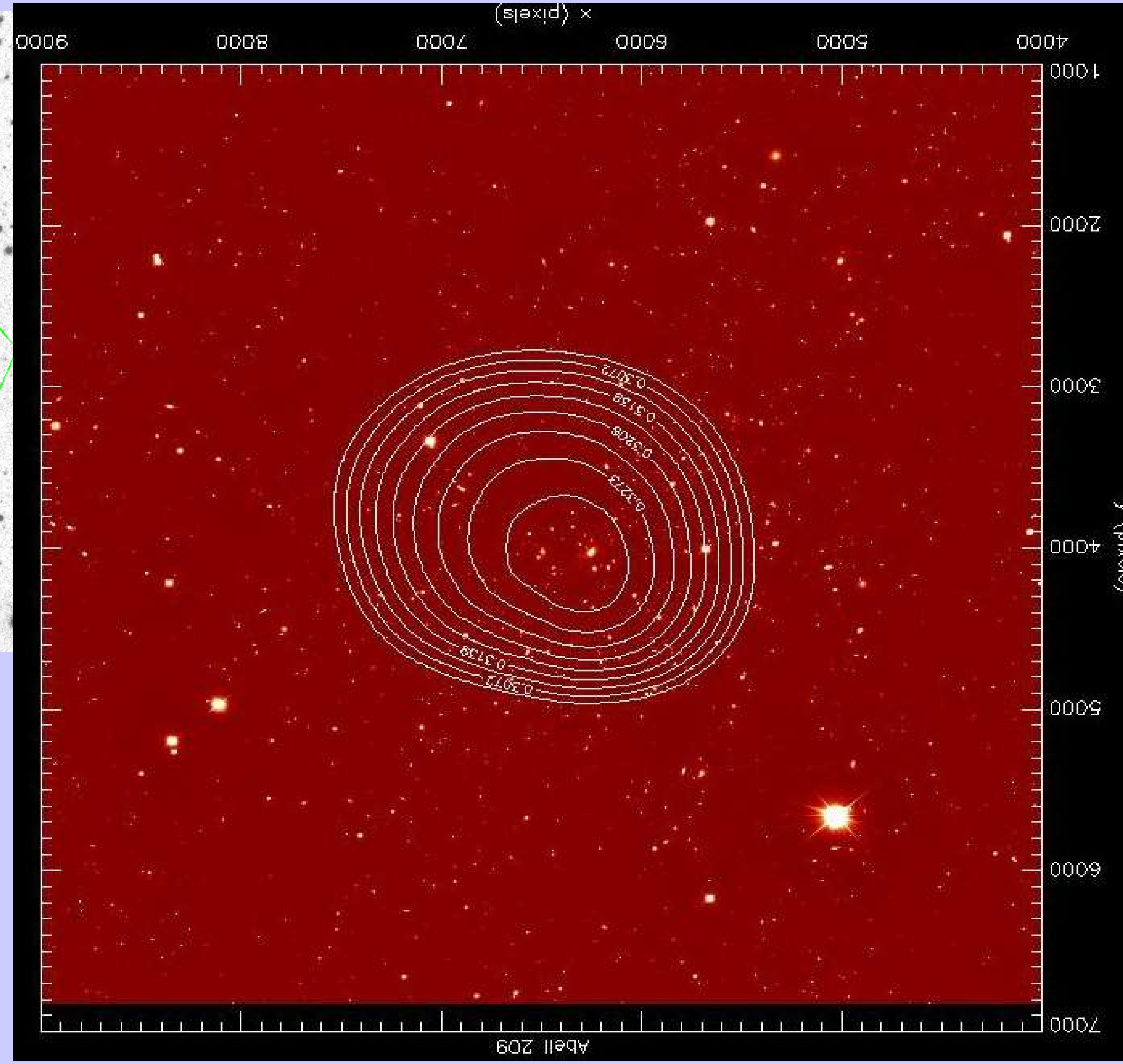

Mercurio et al., 2003

- Consistent with a sum of 2 NFW profiles, 111.5 kpc offset w.r.t. X-ray

Conclusion/Comments/Perspectives

- M_{ap} isocontours do give the mass density but for an additional constant term
- Knowledge of (phot. redshifts) can give the true σ without uncertainties
- WL predicted by *Covariant MOND* (TeVeS, Bekenstein 2004) is not always in agreement with data (Zhao et al., astro-ph/0509590)
- Removal of systematics from Large-Scale Structure in front and behind the Cluster (Ray-tracing simulations + precise models of LSS evolution)

Why is it practically feasible to perform WL analysis?

Because there are plenty of Field Background Galaxies in any cosm. model

- z > 1 angul. size increases slightly with distance (*geometric effect*)
- FBGs are dimmer -> HST observations are ideal (atm. turbulence)

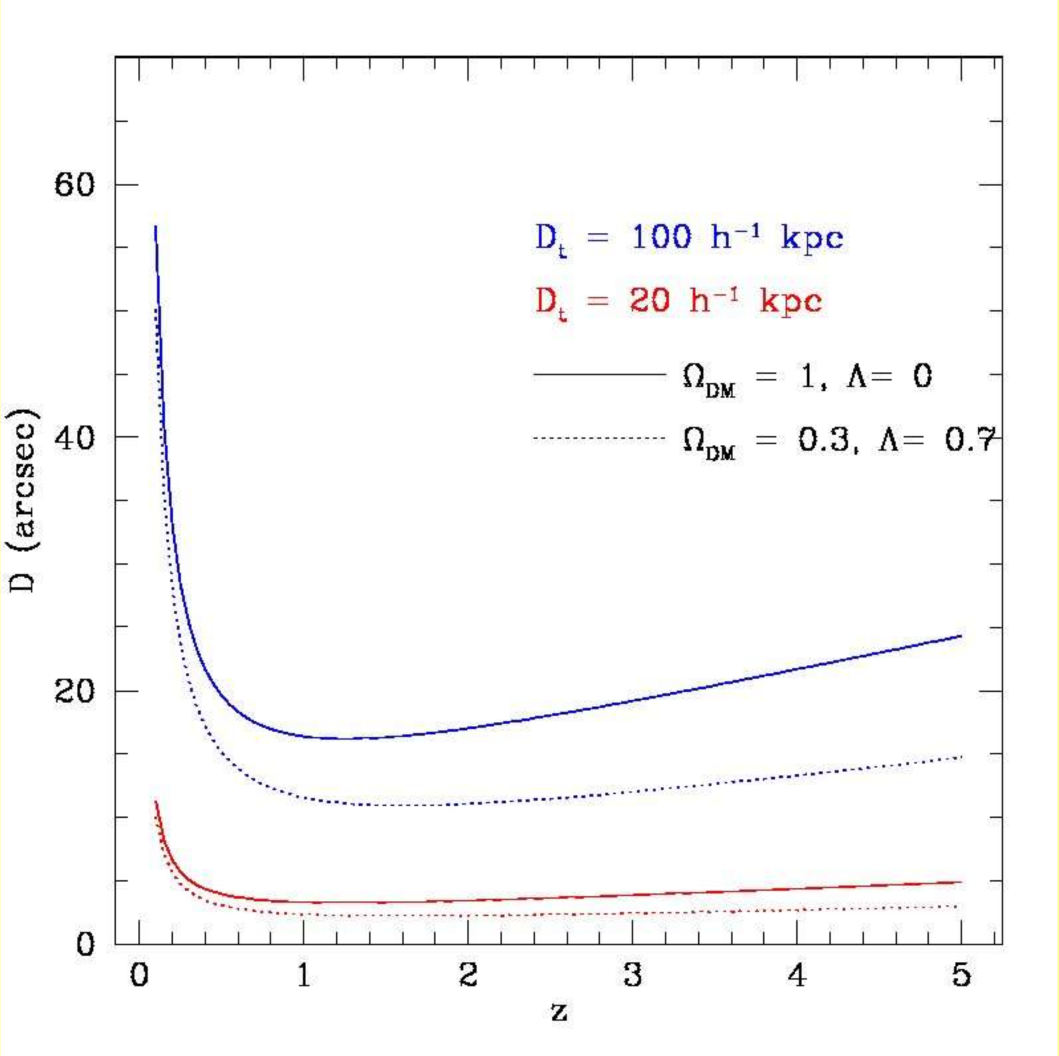

Born Approximation and Multiple planes

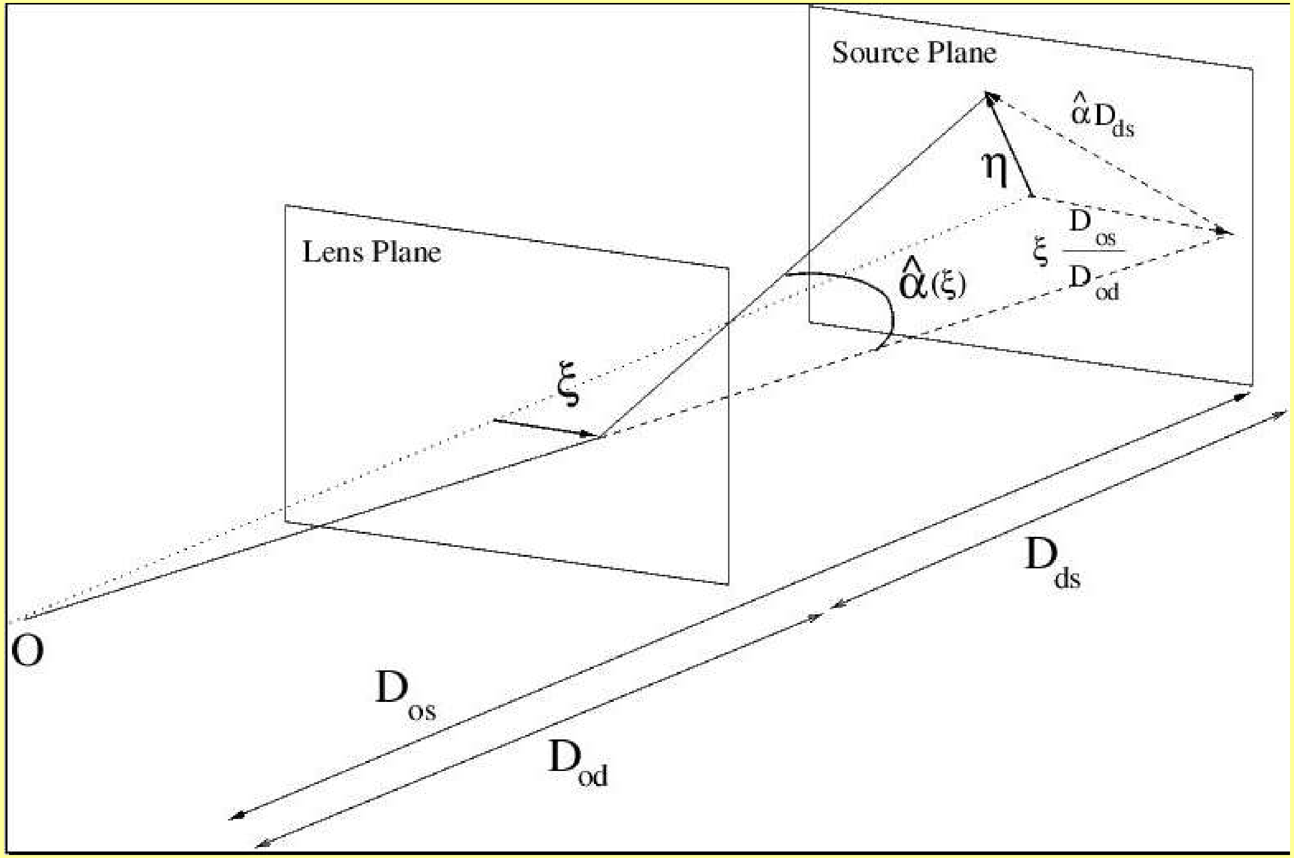

Fluke, Webster and Mortlock (1999)

- BA: deflection=scattering from p.s. $d >> 2GM_s/c^2$
- Mult. planes: 3D mass distr. divided in sequences of 2D planes $\alpha << 1$ i.e. no strong lensing

Ray-tracing equations

- 2D ray tracing equations

->

$$\psi_p = -\frac{2G}{c^2}\int_{\chi_p}^{\chi_p+\Delta\chi} \Phi d\chi$$

$$\theta_n = \sum_{p=1}^{n-1} \frac{r(\chi_n - \chi_p)}{r(\chi_n)} \nabla_\perp \psi_p + \theta_1$$

$$\mathcal{P}_n = \mathcal{I} + \sum_{p=1}^{n-1} \mathrm{g}_{pn} \mathcal{U}_p \mathcal{P}_p$$

$$\mathrm{g}_{pn} = \frac{r(\chi_n - \chi_p) r(\chi_p)}{r(\chi_n)}$$

SHEAR: $\mathcal{P}_p = \frac{\partial \boldsymbol{\alpha}_p}{\partial \boldsymbol{\alpha}_1}$

Cosm. Model - geometry

$$(\mathcal{U})_{ij} = -\frac{2G}{c^2}(\nabla_\perp \nabla_\perp \Phi)_{ij}, Tr(\mathcal{U}) \equiv \Delta\Phi = \frac{3}{2} H_0^2 \Omega_{\mathrm{DM}} \delta$$

Gravitational space-time deform. (newtonian appr.)

Iterative solution for shear:

$$\mathcal{P}_n = \mathcal{I} + \cdots + \sum_{p=1}^{n-1}\sum_{k=1}^{p-1}\sum_{l=1}^{k-1} g_{pn}g_{pk}g_{kl}\mathcal{U}_p\mathcal{U}_k\mathcal{U}_l + \cdots + g_{pn}g_{nk}g_{kl}\cdots g_{j1}\mathcal{U}_n\mathcal{U}_k\mathcal{U}_l\cdots\mathcal{U}_1\mathcal{P}_1$$

propagator

- Decompose the grav. signal into linear+nonlinear part

$$\mathcal{U} \equiv \mathcal{U}^{LSS} + \mathcal{U}^{signal}, \quad \mathcal{U}^{signal} \gg \mathcal{U}^{LSS}$$

$\mathcal{U}^{LSS}$ random correlated matrices

$\mathcal{U}^{signal}$ highly localised on some planes

- *Derive conditions on initial* α *to avoid "chaotic" deviations*

Ray Tracing simulations of WL

Shoot light rays and follow their null geodesics through
a series of LSS realisations (from N-body or MC simulations)

- Our approach: use the TREE of the N-body treecode as a map of the RT algorithm.

PROS:

- Adaptivity - more resol. where mass is more structured
- Memory optimised

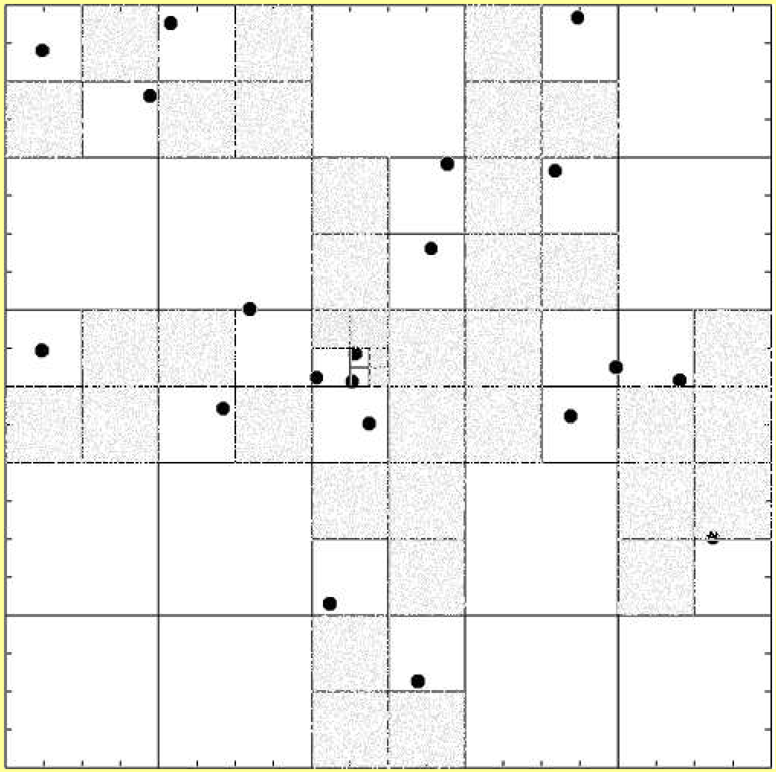

CONS:

- NOISY maps -> post simulation smoothing to match finite resolution

Tracing Filaments with WL

- Main hypotheses:

1) $n_{bkg,gal} = 30$ arcmin^{-2}

2) $<e> = 0.25$, gauss. distr.

- Examples

- $L_{box} = 60\ h^{-1}$ Mpc, z = 0.1

constrained IC, > 5 x 10^6

rays shooted

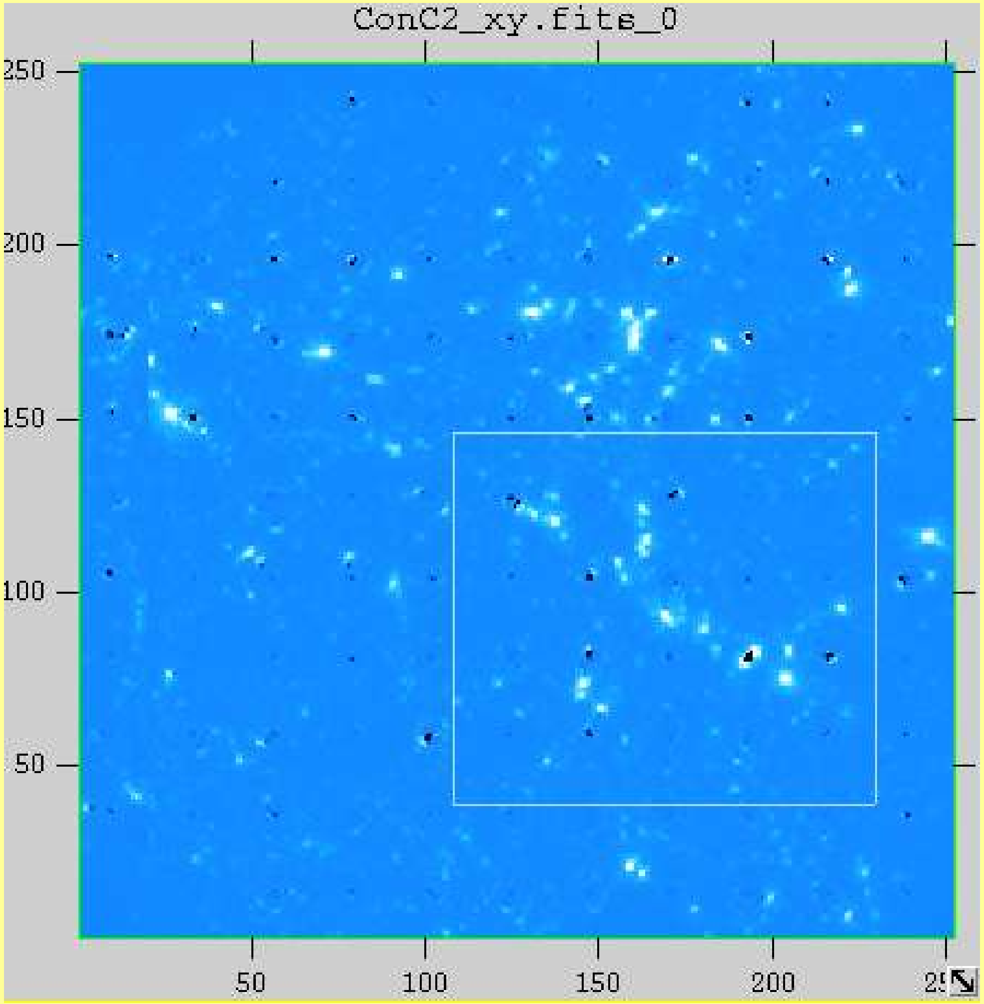

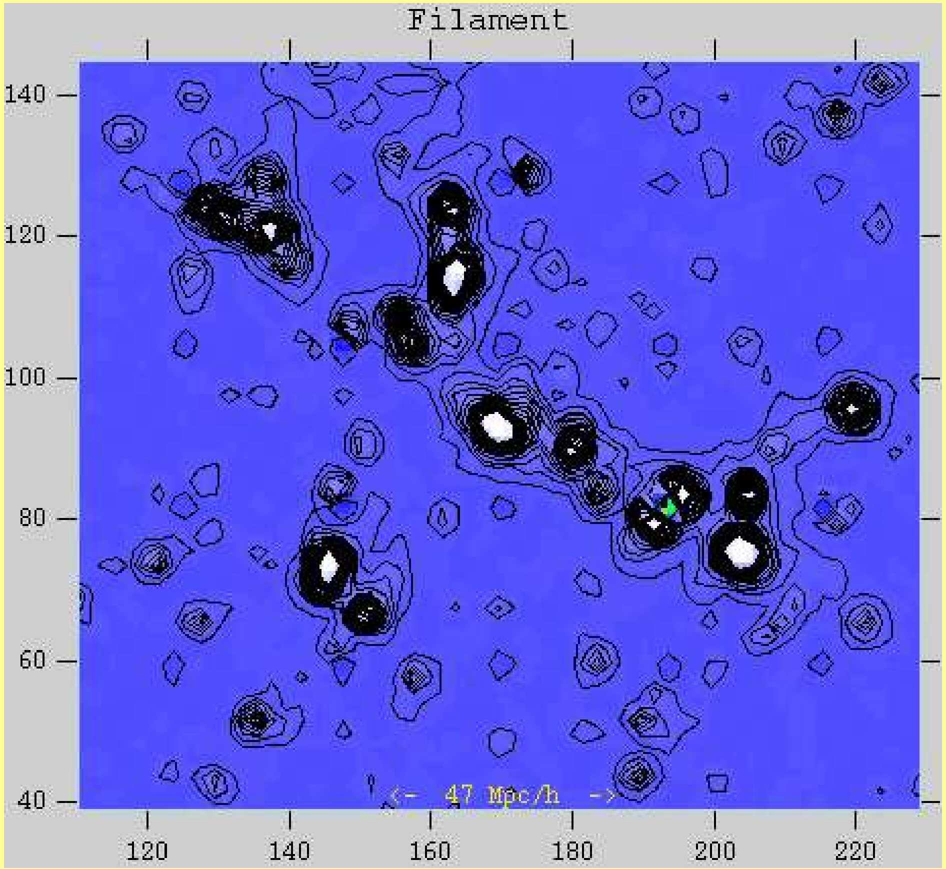

- Filament is few degrees large - massive halos trace it σ_v = 325 km/sec

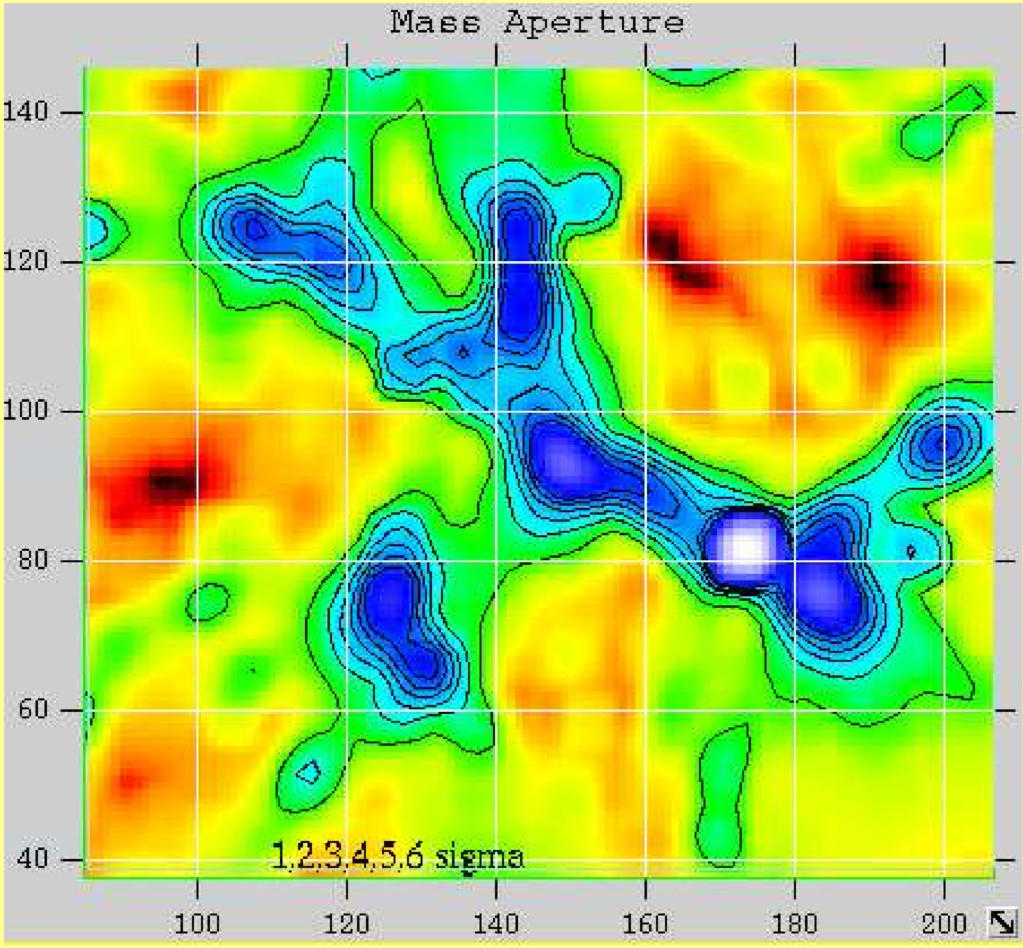

- M_{ap} and S/N contours (Schneider, 1996) - The structure is correctly recovered

False detections

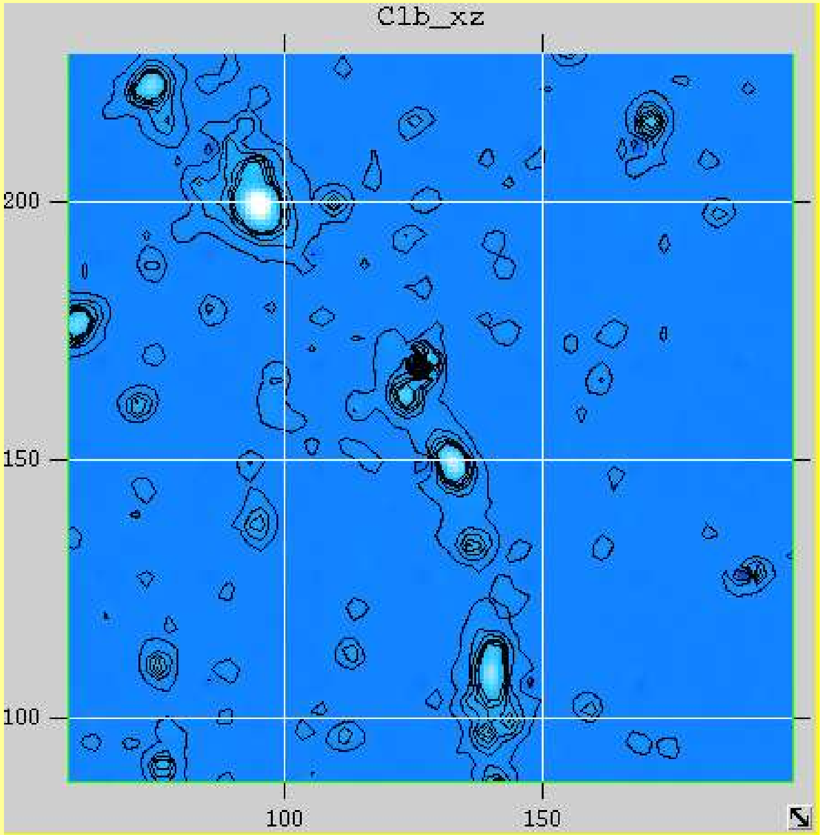

- However, chance alignments can result in unphysical signals

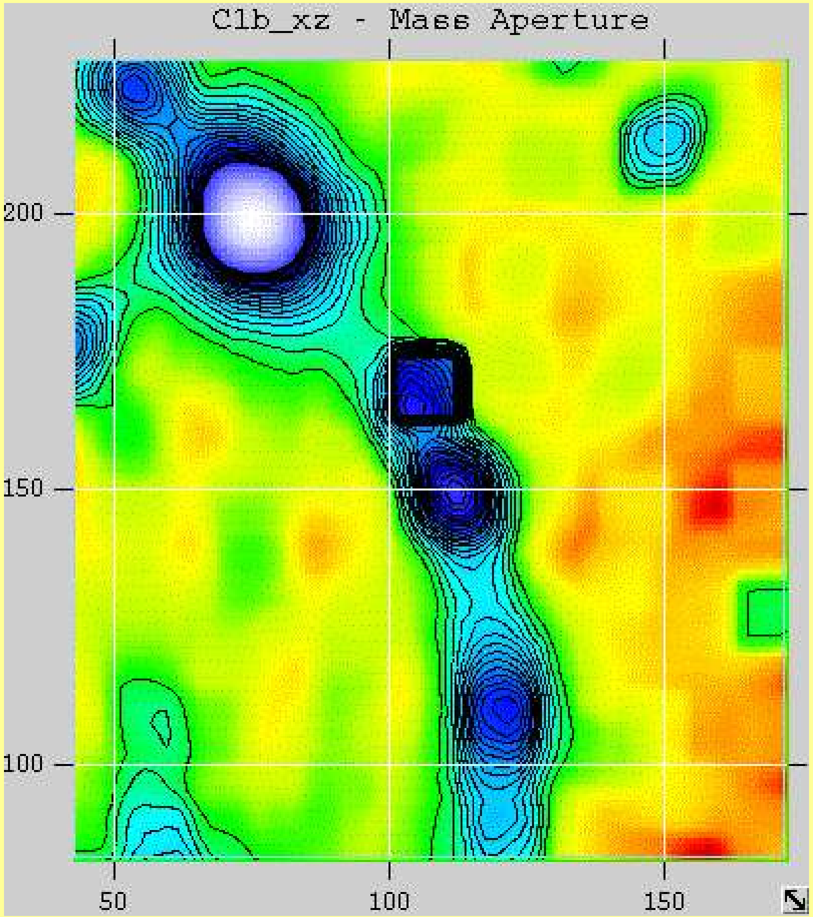

- Tomography can hardly help when nearby massive galaxies dominate the weak signal

Weak Lensing

- The expected statistics

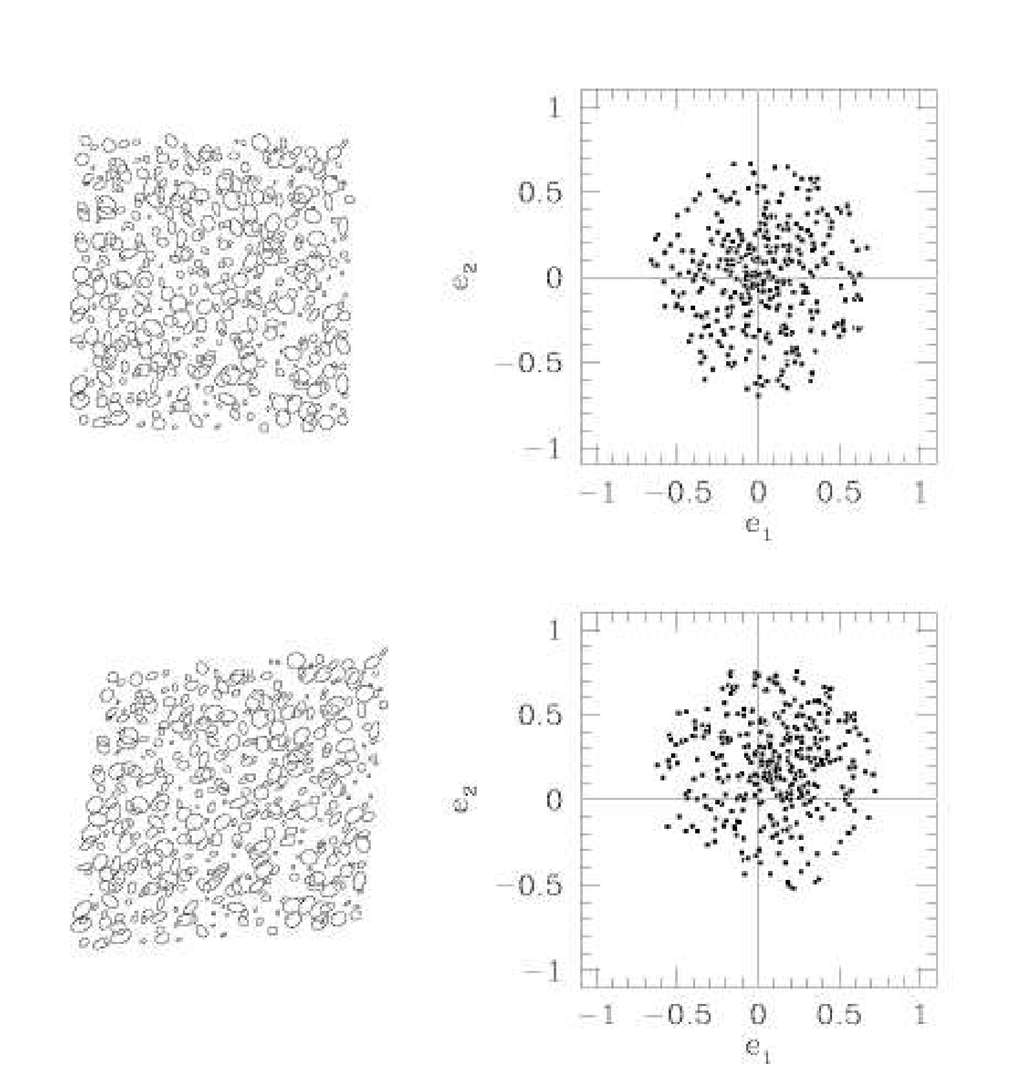

- Signal-to-noise for shear (Bartelmann & Schneider 2001):

$$= 12.7\left(\frac{n}{30\,\mathrm{arcmin}^{-2}}\right)^{1/2}\left(\frac{\sigma_\varepsilon}{0.2}\right)^{-1}\left(\frac{\sigma_v}{600\,\mathrm{km\,s}^{-1}}\right)^{2}\left(\frac{\ln(\theta_{\mathrm{out}}/\theta_{\mathrm{in}})}{\ln 10}\right)^{1/2}\left\langle\frac{D_{\mathrm{ds}}}{D_{\mathrm{s}}}\right\rangle .$$

σ_c = 400 km/sec -> S/N ~ 5.6 (e.g. Eisenstein et al., 1997)